INVESTIGATION OF THE EFFECT OF PARAMETER LEVELS ON EXPERIMENTAL RESULTS IN DRILLING PROCESSES

2023
MASTER THESIS
MECHANICAL ENGINEERING

Safa Aisa Sasi ALGHATOUS

Thesis Advisor
Asst. Prof. Dr. Cevat ÖZARPA

INVESTIGATION OF THE EFFECT OF PARAMETER LEVELS ON EXPERIMENTAL RESULTS IN DRILLING PROCESSES

Safa Aisa Sasi ALGHATOUS

Thesis Advisor
Asst. Prof. Dr. Cevat ÖZARPA

T.C.
Karabuk University
Institute of Graduate Programs
Department of mechanical Engineering

Prepared as
Master Thesis

KARABUK
January 2023

I certify that in my opinion the thesis submitted by Safa Aisa Sasi ALGHATOUS titled "INVESTIGATION OF THE EFFECT OF PARAMETER LEVELS ON EXPERIMENTAL RESULTS IN DRILLING PROCESSES" is fully adequate in scope and in quality as a thesis for the degree of Master of Science.

Assist. Prof. Dr. Cevat ÖZARPA .....
Thesis Advisor, Department of Mechanical Engineering

This thesis is accepted by the examining committee with a unanimous vote in the Department of Mechanical Engineering as a Master of Science thesis. Jan 25, 2023.

Examining Committee Members (Institutions)	Signature
Chairman : Assoc. Prof. Dr. Muhammet Hüseyin ÇETİN (KTUN)	.....
Member : Assoc. Prof. Dr. Harun ÇUĞ (KBU)	.....
Member : Assist. Prof. Dr. Cevat ÖZARPA (KBU)	.....

The degree of Master of Science by the thesis submitted is approved by the Administrative Board of the Institute of Graduate Programs, Karabuk University.

Prof. Dr. Müslüm KUZU .....
Director of the Institute of Graduate Programs

"I declare that all the information within this thesis has been gathered and presented in accordance with academic regulations and ethical principles and I have according to the requirements of these regulations and principles cited all those which do not originate in this work as well."

Safa Aisa Sasi ALGHATOUS

ABSTRACT

Master Thesis

INVESTIGATION OF THE EFFECT OF PARAMETER LEVELS ON EXPERIMENTAL RESULTS IN DRILLING PROCESSES

Safa Aisa Sasi ALGHATOUS

Karabük University
Institute of Graduate Programs
Department of mechanical Engineering

Thesis Advisor:
Assist. Prof. Dr. Cevat ÖZARPA
January 2023, 79 pages

Drilling is a machining operation used to produce holes. This type of machining is frequently employed while creating tools and dies. Additionally, obtaining appropriate results in relation to surface roughness and cutting forces is essential for manufacturing quality. By Taguchi's experimentation method, this thesis investigated two different designs of drilling machining parameters to hole AISI 403 using a computer numerical control machine for the drilling with a solid carbide drill. Experimental drilling of stainless steel AISI 403. The goal of this study was to investigate how cutting parameters affected chip formation, thrust force, and torque. An experimental setup of the first experiments drilling group (Cutting speeds of 512, 640, and 768) with feed-rates of 0.13, 0.17, and 0.2 mm/min. An experimental setup of the second experiments drilling group feed-rates of 0.13, 0.22, and 0.3 mm/min and cutting speeds of 774, 1270, and 1766 rpm. with a carbide drill was a diameter of 10 mm and the coolant. Different chip forms of feed were discovered; The best performances were by two in

the first group and one in the second group. However, it was discovered that both cutting speed and feed-rate had an impact on the average surface roughness of the holes. In the first and second groups, the average surface roughness decreased as the cutting speed increased and the feed rate decreased. Additionally, the rise in feed-rate to a notable rise in the Force-Mean (Fz) and Moment-Mean (Mz). In general, following analysis of surface roughness Ra, Fz, and Mz. results using the statistical software Minitab. It was discovered that both cutting speed and feed rate had an impact on the average surface roughness of the holes. In the first and second groups, the average surface roughness decreased as the cutting speed increased

Keywords **:** AISI304, Drilling, Speed, Feed rate, Cutting speed, Tool Force, Taguchi, Force-Mean, Moment-Mean, ANOVA.

Science Code : 91438

ÖZET

Yüksek Lisans Tezi

DELME İŞLEMLERİNDE PARAMETRE SEVİYELERİNİN DENEYSEL SONUÇLAR ÜZERİNDEKİ ETKİSİNİN İNCELENMESİ

Safa Aisa Sasi ALGHATOUS

Karabük Üniversitesi
Lisansüstü Eğitim Enstitüsü
Makine Mühendisliği Anabilim Dalı

Tez Danışmanı:
Dr. Öğr. Üyesi Cevat ÖZARPA
Ocak 2023, 79 sayfa

Delme işlemi, mühendislik malzemelerinde delik oluşturmak için kullanılan bir talaşlı imalat yöntemidir. Delme ile talaşlı imalat işlemi, takımlar ve kalıplar oluşturulurken sıklıkla kullanılır. Ayrıca, yüzey pürüzlülüğü ve kesme kuvvetleri ile ilgili uygun değerlerin elde edilmesi üretim kalitesi için çok önemlidir. Bu tezde Taguchi yöntemi kullanılarak delme işlemi parametrelerinin iki farklı tasarımı araştırılmış ve farklı parametre seviyelerinin sonuç parametrelerine etkisi analiz edilmiştir. Çıkış parametresi olarak kesme parametrelerinin talaş oluşumunu, itme kuvvetini ve torku nasıl etkilediği araştırılmıştır. İlk deney grubunda 10 mm çapındaki karbür matkap ile, üç farklı kesme hızı (512 rpm, 640 rpm ve 768 rpm), üç farklı ilerleme hızı (0,13 mm/dk, 0,17 mm/dk ve 0,2 mm/dk) parametreleri kullanılmıştır. İkinci deney grubunda ise 10 mm çapındaki karbür matkap ile üç farklı kesme hızı (774 rpm, 1270 rpm ve 1766 rpm) ve üç farklı ilerleme hızı (0,13 mm/dk, 0,22 mm/dk ve 0,3 mm/dk) parametreleri kullanılmıştır. En iyi performans birinci grupta iki numara deneyler,

ikinci grupta ise bir numaralı deney olarak gerçekleşmiştir. Birinci ve ikinci deney gruplarda, kesme hızı arttıkça ve ilerleme hızı azaldıkça ortalama yüzey pürüzlülüğü azalmıştır. Ek olarak, ilerleme hızındaki artış, kuvvet ortalama değerinde (Fz) ve moment ortalama değerinde (Mz) kayda değer bir artışa neden olmuştur. Yüzey pürüzlülüğü (Ra), Fz ve Mz sonuçları istatistiksel yazılım Minitab kullanılarak analiz edilmiştir. Hem kesme hızının hem de ilerleme hızının deliklerin ortalama yüzey pürüzlülüğü üzerinde etkisi olduğu ortaya çıkmıştır. Birinci ve ikinci gruplarda, kesme hızı arttıkça ortalama yüzey pürüzlülüğü azalmıştır.

Anahtar Kelimeler : AISI304, Delme, Hız, İlerleme hızı, Kesme hızı, Takım Kuvveti, Taguchi Kuvvet-Ortalama, Moment-Ortalama, ANOVA.

Bilim Kodu **:** 91438

ACKNOWLEDGMENT

First of all, I want to thank Allah for all of his amazing blessings, especially my good health, my education, and my patience.

I want to dedicate this achievement to my father's soul, who was my best friend and most magnificent tutor, he was credited with everything I accomplished after Allah. Also, I want to thank my mother, who is the source of my life's light.

As I would like to express my deep gratitude, thanks, and sincere appreciation to my supervisor Assist. Prof. Dr. Cevat ÖZARPA for his supervision, and guidance throughout all thesis stages.

And I want to express my profound gratitude to Assoc. Prof. Dr. Muhammet Hüseyin ÇETİN for his assistance in completing the requirements of the thesis.

Last but not least, I must express my sincere thanks to my husband and family for their unwavering support and never-ending encouragement during my years of study. Without them, it would not have been feasible to complete this task.

CONTENTS

Page

APPROVAL ii
ABSTRACT iv
ÖZET vi
ACKNOWLEDGMENT viii
CONTENTS ix
LIS OF FIGURES xiii
LIST OF TABLES xv
SYMBOLS AND ABBREVIATIONS INDEX xvi

PART 1 1
INTRODUCTION 1
1.1. DRILLING MACHINES. 2
1.1.1. Drilling Machine Types. 3
1.1.1.1. Sensitive Drilling Machine. 3
1.1.1.2. Vertical Or Pillar Drilling Machine. 4
1.1.1.3. Radial Drilling Machine. 4
1.1.1.4. Gang Type Drilling Machine. 5
1.1.1.5. Multi-Spindle Machine. 6
1.1.1.6. Numerically Control Machine (CNC). 7
1.1.1.7. Special Purpose Drilling Machine. 7
1.2. DRILLING TOOLS. 8
1.2.1. Carbide Twist Drill. 8
1.2.2. Geometry of a Twist Drill. 9
1.3. MINITAB SOFTWARE IN GENERAL 10
1.4. AISI 304 STAINLESS STEEL. 11
1.4.1. Chemical Composition. 11
1.4.2. Standards. 11
1.4.3. Machinability. 12
1.4.4. Application. 12

Page

PART 2 13
LITERATURE REVIEW 14
2.1. AIM OF THE STUDY 19

PART 3 21
METHODOLOGY 21
3.1. INTRODUCTION. 21
3.2. WORK PLAN. 21
3.2. RAW MATERIAL. 23
3.2.1. Sample Design. 23
3.3. TOOLS. 24
3.4. CALCULATION SPEED AND FEED. 24
3.4.1. Calculation Speed and Feed of The First and Second Group. 25
3.5. EXPERIMENTAL DESIGN USING TAGUCH METHOD. 27
3.5.1. Experimental Design of the first group. 27
3.5.2. Experimental Design of the second group 28
3.6. EXPERIMENTAL WORKS 28
3.7. SURFACE ROUGHNESS MEASUREMENT 32
3.8. USB MIKROSKOP. 32

PART 4 33
RESULTS AND DISCUSSION 33
4.1. INFLUENCE OF MACHINING PARAMETERS ON CHIP FORMATION DURING DRILLING OPERATION. 33
4.1.1 Explanation of experiments of first group chip. 33
4.1.2 Explanation of experiments of second group chip 35
4.1.3 Comparison between first and second group chips 36
4.3. SURFACE ROUGHNESS MEASUREMENTS (Ra) 37
4.3.1. Results of Surface Roughness Ra of First Group. 38
4.3.2. Results of Surface Roughness Ra of Second Group. 39
4.3.3. Comparison Between Ra Results of First and Second Group. 39
4.4. TOOL FORCE 40
4.4.1. Tool Force of The First Group 40

Page

4.4.2. Tool Force of the Second Group 41
4.4.3. Comparison Between the Average Main Force of the First and Second Group Experiments. 42
4.5. ANALYSIS RESULTS USING MINITAB SOFTWARE. 43
4.5.1. Analysis Variance Using ANOVA. 43
4.5.2. Ra Results Analysis of First Group Using ANOVA. 44
4.5.3. Ra Results Analysis of Second Group Using ANOVA. 44
4.5.3. Comparison Between First and Second Groups of Ra Results Analysis Using ANOVA. 45
4.5.3. Force-mean Analysis of First Group Using ANOVA. 45
4.5.4. Force-mean Analysis of Second Group Using ANOVA. 46
4.5.5. Moment-Mean Analysis of First Group Using ANOVA. 47
4.5.6. Moment-Mean Analysis of Second Group Using ANOVA. 48
4.5.7. Comparison Between First and Second Groups of Force-mean and Moment-Mean Results Analysis Using ANOVA. 48
4.6. TAGUCHI METHOD ANALYSIS. 49
4.6.1. Ra Analysis of First Group Using Taguchi Method. 49
4.6.2. Ra Analysis of Second Group Using Taguchi Method. 50
4.6.3. Comparison Between Ra Taguchi Analysis of First and Second Group. 51
4.6.4 Force-mean Analysis of First Group Using Taguchi Method. 51
4.6.5. Force-mean Analysis of Second Group Using Taguchi Method. 52
4.6.6. Moment-Mean Analysis of First Group Using Taguchi Method. 53
4.6.7. Moment-Mean Analysis of Second Group Using Taguchi Method. 54
4.6.8. Comparison Between Force-mean and Moment-Mean Taguchi Analysis of First and Second Group. 56
4.7. 3D SURFACE ILLUSTRATION. 56
4.7.1. 3D Surface Plotter of Ra for First Group. 56
4.7.2. 3D Surface Plotter of Ra for Second Group. 59
4.7.3. Comparison Between 3D Surface Plotter of Ra for First and Second Group 61
4.7.4. 3D Surface Plotter of Force-mean for First Group. 61
4.7.5. 3D Surface Plotter of Force-mean for Second Group. 63
4.7.6. 3D Surface Plotter of Moment-Mean for First Group. 65
4.7.7. 3D Surface Plotter of Moment-Mean for Second Group. 67

Page

4.7.8. Comparison Between 3D Surface Plotter of Fz and Mz for First and Second Group 69

PART 5 70

CONCLUSION AND RECOMMENDATIONS 70

5.1. CONCLUSION 70

5.2. RECOMMENDATIONS 73

REFERENCES 74

RESUME 79

LIST OF FIGURES

Page

Figure 1.1. Sensitive Drilling Machine 3
Figure 1.2. Vertical or Pillar Drilling Machine 4
Figure 1.3. Radial Drilling Machine 5
Figure 1.4. Gang type Drilling Machine 6
Figure 1.5. Multi-Spindle Machine 6
Figure 1.6. CNC drilling machine 7
Figure 1.7. Sum types of Special Purpose Drilling Machine 8
Figure 1.8. Carbide Twist Drill 9
Figure 1.9. Geometry of a Twist Drill 10
Figure 1.10. Minitab version 17 interface 10
Figure 1.11. AISI 304 Application 13
Figure 3.1. Work Plan 22
Figure 3.2. Experimental Sam. 23
Figure 3.3. Workpiece. 23
Figure 3.4. The twist solid carbide drill. 24
Figure 3.5. Speed doctor calculates S&F 24
Figure 3.6. Calculate Speed and Feed 26
Figure 3.7. HAAS VF-2SS milling machine. 30
Figure 3.8. Experimental Works. 30
Figure 3.9. Stationary dynamometer. 31
Figure 3.10. Multichannel charge amplifier. 31
Figure 3.11. Surface Roughness Measuring Device SJ-410 32
Figure 3.12. USB Microscope 32
Figure 4.1. Chip of the First Group. 34
Figure 4.2. Chip of the Second Group 35
Figure 4.3. The chips of experiments number 1,4 and 7(first group). 36
Figure 4.4. The chips of experiments number 1and 5 (second group). 36
Figure 4.5. Surface Roughness Profile 37
Figure 4.6. Surface Roughness Measure 38

Page

Figure 4.7. Ra of the First Group. 38
Figure 4.8. Ra of the second Group. 39
Figure 4.9. Comparison Between Ra of the First And Second Group. 40
Figure 4.10. Force-Time of the first group 41
Figure 4.11. Force-Time of the Second Group. 41
Figure 4.12. Comparison Between The Average Main Force. 43
Figure 4.13. Main Effects Plot for Ra-Avg and SN Ratios of The First Group. 49
Figure 4.14. Residual plots for Ra-Avg of The First Group. 50
Figure 4.15. The Second Group Main Effects for Ra-Avg and SN Ratios. 50
Figure 4.16. Residual plots for Ra of The Second Group. 51
Figure 4.17. Main Effects Plot for Force-mean and SN Ratios of The First Group. . 52
Figure 4.18. Residual plots for Force-mean of The First Group. 52
Figure 4.19. Main Effects Plot for Force-mean and SN Ratios of The Second Group. 53
Figure 4.20. Residual plots for Force-mean of The Second Group. 53
Figure 4.21. Main Effects Plot for Moment-Mean and SN Ratios of The First Group 54
Figure 4.22. Residual plots for Moment-Mean of The First Group 54
Figure 4.23. Main Effects Plot for Moment-Mean and SN Ratios of Second Group 55
Figure 4.24. Residual plots for Moment-Mean of The Second Group. 55
Figure 4.25. 3D Surface Plotter of Ra for First Group. 58
Figure 4.26. 3D Surface Plotter of Ra for Second Group. 60
Figure 4.27. 3D Surface Plotter of Force-mean for First Group. 62
Figure 4.28.3D Surface Plotter of Force-mean for Second Group. 64
Figure 4.29.3D Surface Plotter of Mz for First Group 66
Figure 4.30. 3D Surface Plotter of Mz for Second Group. 68

LIST OF TABLES

Page

Table 1.1. Chemical composition of AISI 304 Stainless Steel 11
Table 1.2. Standards of AISI 304 Stainless Steel 11
Table 3.1. The first group factor Design. 27
Table 3.2. The second group factor Design. 27
Table 3.3. Parameters of the first group. 28
Table 3.4. Parameters of the first group. 28
Table 3.5. CNC Machine specifications 29
Table 4.1. Ra Average of the first group 38
Table 4.2. Ra average results of second group. 39
Table 4.3. Main Force Average of The First Group 41
Table 4.4. Main Force Average of the Second Group 42
Table 4.5. Ra Results Analysis of First Group Using ANOVA. 44
Table 4.6. Ra Model Summary of First Group. 44
Table 4.7. Ra Results Analysis of Second Group Using ANOVA. 45
Table 4.8. Ra Model Summary of Second Group. 45
Table 4.9. Fz Analysis of First Group Using ANOVA. 46
Table 4.10. Fz Model Summary of First Group 46
Table 4.11. Fz Analysis of Second Group Using ANOVA. 46
Table 4.12. Fz Model Summary of Second Group. 47
Table 4.13. Mz Analysis of First Group Using ANOVA. 47
Table 4.14. Mz Model Summary of First Group.. 47
Table 4.15. Mz Analysis of Second Group Using ANOVA. 48
Table 4.16. Mz Model Summary of Second Group.. 48

SYMBOLS AND ABBREVIATIONS INDEX

ABBREVIATIONS

CNC	:	Computer Numerical Controlled
Fn	:	Feed rate
S	:	Speed
Rpm	:	Rotation per minute
Fz	:	Force-Mean
Mz	:	Moment-Mean
Ra	:	Surface Roughness

PART 1

INTRODUCTION

The actual global competitiveness in manufacturing today revolves around finding ways to produce goods of higher quality at lower costs. There is a constant need to lower tooling costs in order to produce things more affordably, particularly when executing machining processes, one of these needs is to lengthen the lifespan of the cutting tool by choosing the suitable cutting parameters which results in reducing surface roughness and cutting forces.[1.3] In this approach, there are many experimental design and methodologies such as Taguchi and Response Surface methods are carried out for the selection of optimum experimental parameters, which is led to significant savings are made in terms of both time and cost. These studies also show that the reliability of the system has not decreased due to the decrease in the number of experiments. A second benefit of experimental design methods is that, the optimum points of (maximum, minimum, nominal) can be determined of Ra and the Force reaction generated by cutting. Therefor and due to the stated benefits, it is important to use experimental design methods in manufacturing-oriented experimental studies. However, while creating the experimental design methodology, the parameter levels should be chosen with a significant difference. In cases where the difference between levels is very close, it is difficult to obtain general information about the system. According to [4] the difference between the levels is increased with significance of the effect ratios of the parameters decreases. In addition, there is no study in the literature on how parameter levels will affect the test results.[5] In this study, two different experimental designs performed and the effect of parameter levels on the test results analyzed. An effective information on the most appropriate parameter level selection obtained. In the first experiment design, the difference between the levels will be kept at a minimum level, and in the second experiment design, the level differences will be kept at the maximum level. Optimization, variance, and regression analysis will be performed for the results obtained from both

experimental designs. The results will be compared and tried to obtain information about the selection of the most suitable parameter levels. If there is a significant difference between the results, an empirical correlation would be obtained for the selection of parameter levels. Drilling is one of operation primary procedures used in the material cutting. In this research, studying will do drilling experiments on AISI 304 Stainless Steel [1,5].

1.1. DRILLING MACHINES

In any workshop, a drilling machine is a powerful piece of equipment. It is intended to create a cylindrical hole with the desired depth and diameter on metal, wood, plastic or any solid workpieces. Nevertheless, holes can be made by different machine tools in a shop, drilling machine is designed specifically to execute the operation of drilling and similar operations. This is considered as frequent machining method; according to one estimate, the drilling operation accounts for 75% of the metal cutting material removed during this process. A chuck holds the cutting instrument known as the drill in the drill press while it is fed into the workpiece at varying speeds. The speed, feed and coolant are all controlled by the special machine for the desired completed part, machine controls must be given. The drilling machine is beneficial for many other machining tasks in addition to being used for drilling. [6,7].

The main construction body of the base, column, drill head, and spindle make up a drilling machine. The base is commonly made of cast iron and may rest on a bench, foundation or floor depending upon the design. Larger and heavy-duty machines are firmly fitted on the ground. The base is where the column is mounted vertically. The table can be positioned on it and is precisely machined. On the top of the column, there are attachments for the drill spindle, an electric motor, and a system for operating the spindle at various speeds. A flat belt or a "V" belt transfers power from the electric motor to the spindle [7].

1.1.1. Drilling Machine Types

There are several types of conventional and digital drilling machine used in manufacturing industry. Some of these popular machines will be described in this research: [8].

- ✓ Sensitive Drilling Machine.
- ✓ Pillar or Vertical Machine.
- ✓ Radial Arm Machine.
- ✓ Gang Type Machine.
- ✓ Multi-Spindle Machine.
- ✓ Numerically Control Machine (CNC).
- ✓ Special Purpose Drilling Machine [9].

1.1.1.1. Sensitive Drilling Machine

A base, column, table, spindle, drill head, and driving mechanism make up a sensitive drilling machine. By means of bolts and nuts, the machine's base is secured to a level surface. The delicate drilling equipment is intended to drill tiny holes quickly in intricate pieces of work. High speed and hand feed mechanisms are essential for drilling small holes. As the drill is fed into the work-piece by hand, the operator will feel the cutting progress of the drill into the workpiece and accordingly he can control the down feed pressure as shown in figure 1.1 [9,10].

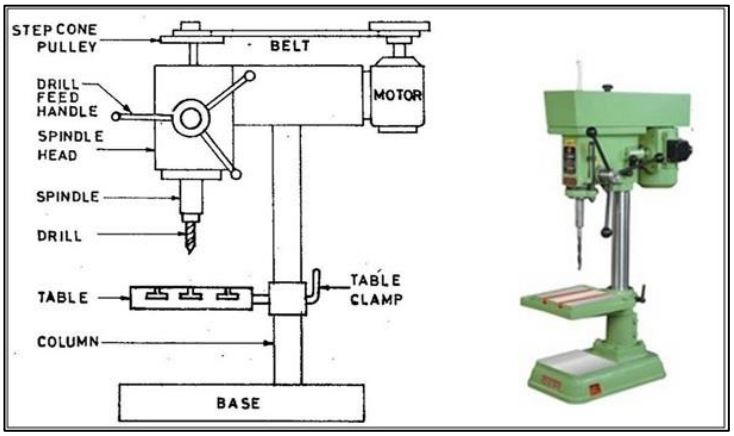

Figure 1.1. Sensitive Drilling Machine [10].

1.1.1.2. Vertical Or Pillar Drilling Machine

Vertical or Pillar Drilling Machine is free standing and it is designed for holding medium sized work-pieces. From the shape, it is almost similar to the sensitive drilling machine, however, it is a larger and heavier structure, which is able to take larger drills. Power speed and feeds are available, and the table height is movable. As shown in figure 1.2.[11], the larger drills often have a tapered shank inside a taper bore at the spindle end.

Figure 1.2. Vertical or Pillar Drilling Machine [12].

1.1.1.3. Radial Drilling Machine

The radial drilling machine is mainly designed for drilling on medium to large and heavy workpieces. It has a heavy round column attached on a large base. The column holds a radial arm, which can be moved up and down. The arm holds the drill head, which can be move around and radial along the arm. These unique features of this type of machine drills, the operator can establish intersecting or angle holds in a single setup by positioning the spindle directly over the workpiece rather than moving the component to the tool, as shown in the figure. 1.3.[13].

Figure 1.3. Radial Drilling Machine [14].

1.1.1.4. Gang Type Drilling Machine

Gang drilling machines mainly designed with a long worktable and a base. As illustrated in the figure 1.4, a number of drill heads or stations are fixed on a single long table. This machine is used for production work. A sequence of operations such as drilling, reaming, counter boring and tapping can be accomplished on a single workpiece by simply shifting this work-piece from one position to the other along the worktable. Here, each spindle is equipped with a specific set of tools for a particular operation [11,13].

Figure 1.4. Gang type Drilling Machine [15].

1.1.1.5. Multi-Spindle Machine

In the multi-spindle drilling machine, a number of spindles are installed on a single head to enable the simultaneous drilling of numerous holes as indicated in the figure 1.5. Here all the spindles holding the drills are fed into the workpiece at the same time. The distances between the spindles can be changed according to the locations where holes are to be drilled. Drill jigs are used to hold the drills [13].

Figure 1.5. Multi-Spindle Machine [16].

1.1.1.6. Numerically Control Machine (CNC)

Computer numerical control can change the tool automatically, as illustrated in figure 1.6, the program regulates the speeds, feeds, and table movement. [17].

Figure 1.6. CNC drilling machine [18].

1.1.1.7. Special Purpose Drilling Machine

These are machines with several spindles for drilling, milling, tapping, boring, and reaming. These machines are designed to perform many operations on a component in a single setting, and as can be seen in figure 1.7, there are numerous types and shapes available. [19].

Figure 1.7. Sum types of Special Purpose Drilling Machine [20].

1.2. DRILLING TOOLS

Drilling tools are cutting tools designed for producing holes in a workpiece. There are many different types of drilling tools so choosing the right drilling tool for a set of jobs is one of the most important skills that should be considered by any operator.

Drills are designed and manufactured in several different sizes and shapes, which are suitable for wood, walls, and metals. In addition to the purpose of use, the material from which the tool is manufactured is different. The common tools are made from the HSS and carbide. This study only considers the carbide twist drill which is the most tool used for hard metals such as stainless steel [21].

1.2.1. Carbide Twist Drill

The twist drill, which is depicted in figure 1.8, is the most typical form of drill used presently. Currently available twist drills are created by milling two spiral grooves or flutes that run lengthwise around the drill's body. There are different sizes of twist drills according to shape, the flute's length, diameter, and the tool's length overall [22].

Figure 1.8. Carbide Twist Drill [23].

1.2.2. Geometry of a Twist Drill

Different geometries severely affect the hole's dimensions precision and the drill's tool life. The geometry of a twist drill can be examined in more detail in order to comprehend which feature of the drill geometry affects which factor for tool life or drill tolerances. Where the tool is divided according to the following as shown in figure 1.9 [24].

- ✓ Point angle
- ✓ Main cutting edges
- ✓ Main flank
- ✓ Secondary cutting edge
- ✓ Chip flute
- ✓ Guide land
- ✓ Side rake angle

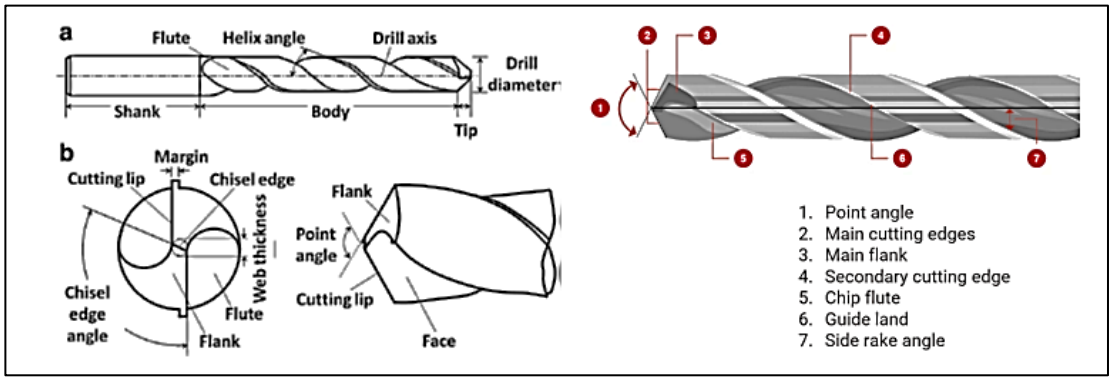

Figure 1.9. Geometry of a Twist Drill [25].

1.3. MINITAB SOFTWARE IN GENERAL

It was created as a multifunctional statistical software package for simple interactive use. In the '70s at Pennsylvania State University, researcher Brian L. et.al developed Minitab. [26]. Minitab is a good choice for educational applications, it is also robust enough to serve as the primary tool for data study. Figure 1.10 shows the interface of Minitab software that it works with Windows. supports factorial, response surface, mixture, and Taguchi designs for experiment design and analysis [26,27].

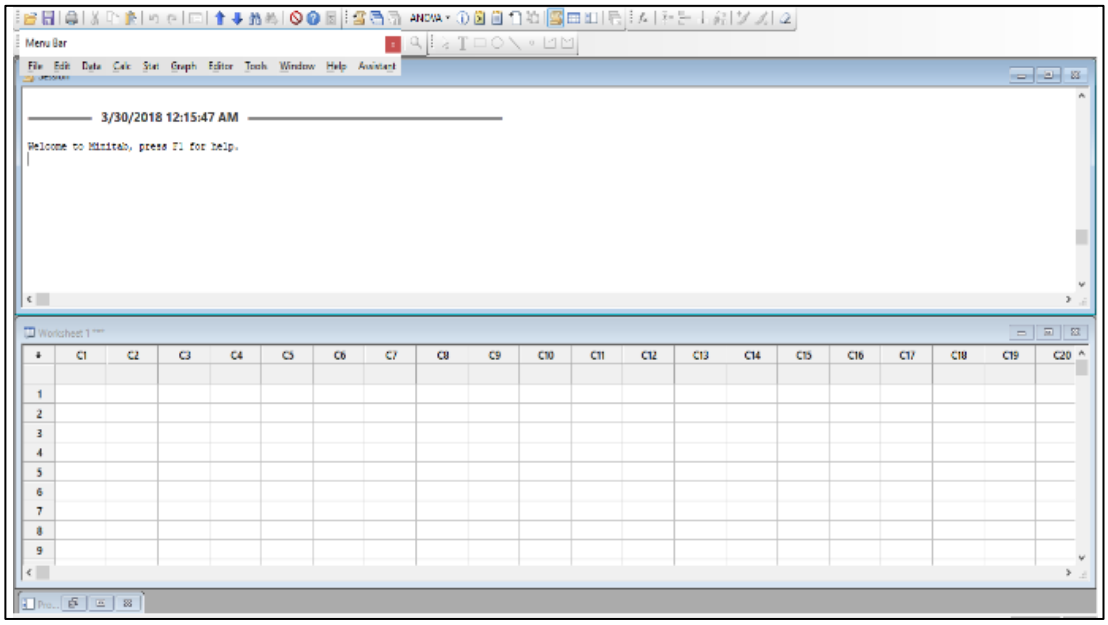

Figure 1.10. Minitab version 17 interface [27].

1.4. AISI 304 STAINLESS STEEL

Austenitic chromium-nickel stainless steel ASTM AISI 304 is a popular material. It is very formable, and it also has strong corrosion resistance. [28].

1.4.1. Chemical Composition

Type 304 is occasionally also mentioned as 18/8, a moniker that comes from its typical composition of 18% chromium and 8% nickel. Other elements in the alloy include nickel, manganese, phosphorus, nitrogen silicon, carbon, and Sulphur Table 1.1 illustrate the chemical composition [29,30].

Table 1.1. Chemical composition of AISI 304 Stainless Steel [30,31].

Composition	**%**
C	≤ 0.07
Si	≤ 1.00
Mn	≤ 2.00
P	≤ 0.045
S	≤ 0.015
Cr	17.5-19.5
Ni	8.00-10.5
N	≤ 0.11

1.4.2. Standards

Standards is concise statements Certified and internationally recognized, especially clarifying the name of the metal. Table 1.2 displayed the Standards of AISI 304 Stainless Steel recognized according to international standards [30].

Table 1.2. Standards of AISI 304 Stainless Steel [30].

Material No.	**EN Designation**	**AISI/SAE**	**UNS**
1.4301	X5CrNi18-10	304	S30400

1.4.3. Machinability

AISI 304 has good machinability but requires a lot of coolants and lubricants, especially on the cutting edges, because to its low thermal conductivity [32].

1.4.4. Application

Typical applications include as shown in figure 1.11.

- ✓ oil industry.
- ✓ Food processing equipment such as milk processing.
- ✓ Tables, troughs, sinks, equipment, and other accessories for the kitchen.
- ✓ Architectural paneling, railings, and trim.
- ✓ Chemical containers, as well as for transport.
- ✓ Heat Exchangers.
- ✓ Woven or welded screens for water filtration, mining, and quarrying.
- ✓ Threaded fasteners.
- ✓ Springs.

Figure 1.11. AISI 304 Application [33,34,35,36].

PART 2

LITERATURE REVIEW

An essential fundamental tool needed for the machining of a manufacturing part is the drilling tool. It does not only performs cutting tasks but also aids in obtaining the required surface finish and product quality. surface quality depends more on the cut parameters which have a positive or negative effect on the cutting. One of the most essential factors that affect how well the parts work is the surface quality. The force of the tool, and thereby on tool life. Therefore, there are many studies carried out in this field.

Mustafa Kurt, Eyüp Bagci and Yusuf Kaynak in 2008 their research focused on using Taguchi techniques to optimize cutting parameters for hole diameter accuracy and surface finish in dry drilling techniques. In this research, the Taguchi method was used to investigate how cutting factors affected the surface finish and hole diameter with highly accurate results during dry drilling of the Al 2024 alloy. The specifications for the drilling process were chosen while taking into account manufacturer and industrial needs. The gotten optimal parameters have been used in drilling processes by the manufacturer [37].

E. Kilickap. In 2010, he developed a Taguchi method application for examining the impact of cutting parameters and point angles on the varying parameters in dry drilling of GFRP composites. First, the analysis of experimental results has been done using Taguchi's orthogonal array and analysis of variance, according to the findings of this study. ANOVA is used to assess the effectiveness of the optimal cutting parameters and point angles on the damage. Secondly, the damage is directly proportional to the cutting parameters, which means that the composite damage is greater than the high cutting speed and feed rate. Finally, the feed rate is the primary cutting parameter that has the greatest impact on the delamination factor for both drills, based on ANOVA data. moreover, low feed rates caused less damage [3].

In 2012, Adem Çiçek, et.al. tested how drilling settings and deep cryogenic treatment affected surface roughness and roundness error when drilling AISI 316 austenitic stainless steel using M35 HSS twist drills. Moreover, the Taguchi technique was used to identify the best control variables for hole quality. Cutting speeds, feed rates, and two cutting tools were taken into consideration as control parameters, and L8 orthogonal array was chosen for testing purposes. The prediction equations of the surface roughness and roundness error achieved from the experimental design were derived via multiple regression analysis. With treated drills, the lowest surface roughness and roundness error were recorded at 14 m/min cutting speed and 0.08 mm/rev feed rate. Confirmation results reported that, while drilling stainless steel, the Taguchi approach precisely improved the drilling parameters. [39].

In 2012 B. Ramesh and A. Elayaperumal had studied to optimization of process parameter levels during drilling using coated solid carbide twist drill. An analysis of variance (ANOVA) was used to examine the effects of process variables including feed and spindle speed on thrust force and torque during drilling using Taguchi's orthogonal array. To obtain defect-controlled drilling, the process parameters were optimized for the minimum thrust force and lowest torque. Using the statistical program MINITAB 15. Correlations between thrust force and torque and process factors were determined. Among the process parameters examined, feed significantly affects both the thrust force and torque with 88.52% and 92.83% respectively while the impact of spindle speed on the above was moderately insignificant [40].

K. Lipin and P. Govindan in 2013 their research focused on using Taguchi methods for multi-objective improvement of drilling parameters. In order to get improved performance characteristics, the Taguchi method has been used to determine the main effects, significant factors, and best machining conditions, surface roughness, cutting force, and tool life. It was detected that the optimal speed for a machine tool is influenced by various processing parameters such as hardness, composition, stiffness of work/tool and tool life. Additionally, it’s clear that the feed is strongly affected by the need for surfaces to be finished. The input parameters, workpiece or tool material, and machine tool condition have a significant impact on the roughness of drilled surfaces [41].

H. Prakash (2014) studied the twist drill. This study discussed an application of the Taguchi method for investigating the effects of cutting parameters on the surface finish in the drilling process of SG Iron. The analysis of the experiments for surface finish has Shown that Taguchi's parameter design can successfully Verify the optimum cutting parameters [42].

Palanisamy Shanmughasundaram and Ramanathan Subramanian in 2014 Study of parametric optimization of burr development in step drilling of eutectic Al-Si alloy-Gr composites were the focus of their research. In order to investigate the impacts of the step drill's geometries and cutting parameters on the exit burr height in drilling of Al-Gr, the Study provided an application of L27 orthogonal array of Taguchi technique and analysis of variance. According to this study, the following conclusions have been summarized. According to the ANOVA results, the most important factors affecting the exit burr height were spindle speed, step size, step angle, and feed. Feed was found to have a significant influence on thrust force. Unusually, the results showed that increasing the feed increased the thrust force and burr height. The Taguchi experimental design technique can be used successfully for both optimization and prediction, as illustrated by the similarity between the results of predictions based on calculated S/N ratios and experimental values. [43].

J. Udaya Prakash and Perumal Sudalai in 2015 their study was about the Optimization of Machining Parameters in the Drilling of Aluminium Matrix Composites using the Taguchi Technique, experimental results demonstrated optimization of the drilling process parameters of AMCs and Feed rate is the parameter that has the highest statistical influence on thrust force values of the composites (53.98%) followed by material (13.78%), drill type (10.53%) and spindle speed (8.37%). Also, the pooled error associated with the ANOVA is 4.12% for the factors showing a 95% confidence level and the confirmation experiments show that the error related to thrust force is negligible [44].

In 2017 A.T. Kuzu, K. Rahimzadeh Berenji, B.C. Ekim and M. Bakkal studied the thermal modeling of the deep-hole drilling process under MQL, for chip removal, the heat load fluctuation along the cutting lip, the chisel, and the margin, as well as the

heat convection of the oil-air combination, the workpiece's heat distribution was estimated. The largest heat flow is found by analysis of the results to be near the chisel edge, with a diminishing trend along the cutting lip from the chisel to the drill bit's periphery. When the cutting speed increased from 25 to 50 m/min under the same feed values, the heat energy was twice as high, despite the fact that the thrust force and torque values were equal [45].

In 2018 Güven Meral,et.al. To enhance the performance of hole drilling, new drill geometries were designed and manufactured after surface roughness, thrust force, and torque produced by these geometries were investigated using Taguchi-based GRA. Surface roughness, thrust force, and drilling torque were used to evaluate the drills' performance. Four alternative drill geometries, four levels of cutting speed, and four levels of feed rate were chosen for the performance test. On the material, AISI 4140, holes were drilled. The optimization process also included two steps. First, Taguchi's S/N analysis was used to do a mono-optimization in which each performance output was optimized separately [46].

Aseel Jameel Haleel in 2018. Her research focused on improving the efficiency of drilling parameters using the Taguchi approach to achieve the ideal surface roughness value when using HSS twist drills to drill Aluminium alloy grade 5050. The optimum drilling conditions at a level were successfully determined by the proposed Taguchi method, S/N ratio, and ANOVA (5). From S/N ratio result based on ranking and ANOVA result based on F- value the tool diameter is the most significant control factor follow by feed rate and the cutting speed has the least significant on surface roughness [47].

In 2018 J. Pradeep Kumar and P. Packiaraj had discussed the effect of drilling parameters on surface roughness, tool wear, material removal rate and hole diameter error in drilling was an application of Taguchi method for investigating the effects of drilling parameters on surface roughness, tool wear, material removal rate and hole diameter error in the drilling, and analysis of results in the drilling process using conceptual Signal-to-Noise(S/N) ratio approach, regression analysis, and analysis of variance (ANOVA) so statistically designed experiments based on Taguchi method

are performed using L18 orthogonal array to analyze the effect of drilling parameters on surface roughness, tool wear, material removal rate and hole diameter error. Linear regression equations are developed to predict the values of surface roughness, tool wear, material removal rate and hole diameter error and the predicted values are compared with measured values. and Through ANOVA, it is found that the feed and speed are important process parameters to control surface roughness, tool wear, material removal rate and hole diameter error [48].

C Sarala Rubi, J Udaya Prakash, and C Rajkumar (2020) their research focused on process parameter optimization by applying the Taguchi technique for drilling Aluminium matrix composites. The experiments were carried out in a CNC vertical machining center equipped with a cutting tool dynamometer to measure the thrust force, and a vision measurement system to measure burr-height. Experimental results demonstrated that this strategy enhances the performance characteristics expected in the drilling phase [49].

Muhammad Aamir, Shanshan Tu, Majid Tolouei-Rad, Khaled Giasin and Ana Vafadar in 2020 their study was about the optimization and Modelling of Process Parameters in multi-hole simultaneous drilling using Taguchi method and fuzzy logic approach. With a poly-drill head, drilling experiments were conducted using one-shot drilling and multi-hole simultaneous drilling. Process parameter optimization for better hole quality in terms of surface roughness and hole size was done using the Taguchi method. Regression analysis and ANOVA were then used to validate the model's accuracy and the importance of the process parameters. In addition, a fuzzy logic technique was used to anticipate surface roughness and hole size when drilling multiple holes with a poly-drill head. It came to an end. Cutting speed and feed rate significantly affect both types of drilling processes while drilling Al5083. Additionally, it is hypothesised that additional vibration will probably be present as a result of the tool's rotating motion. Additionally, when the feed rate increases, the size of the chips also does. Therefore, both the surface roughness and hole size might be impacted by a greater cutting speed and feed rate. According to the ANOVA results, cutting speed and feed rate have an impact on surface roughness and hole size for both types of drilling, respectively. It was demonstrated that the Taguchi approach can

effectively analyse the ideal process parameter combination for surface roughness and hole size, as accomplished in multi-hole drilling with a decreased cutting speed and feed rate [50].

In 2022 Tarun Sahu and Kamlesh Gangrade studied optimization of cutting parameters to reduce the surface roughness by taguchi method. They came to the conclusion that feed rate, which affects practically all machining processes, including drilling, milling, turning, and reaming, is the most essential and dominant parameter for surface roughness. When drilling, feed rate and spindle speed had a beneficial influence on surface roughness; when turning, feed rate with cutting speed and depth of cut did. [51].

Md Shahrukh Khan and Dr. Shahnawaz Alam in 2022 their study was about a study of the impact of multiple drilling parameters on surface roughness, tool wear and material removal rate while drilling al6063 applying Taguchi technique. The tool's wear was measured, The material cleans the workpiece of aeration, and While drilling Al 6063 alloy with an HSS spiral tool, the rate of feeding, the rotation speed of the tool, and the diameter of the tool are used as input process parameters to measure the surface roughness of the sample at the entry and exits of the work material to improve the quality of the hole while drilling Al 6063 alloy, drilling conditions are altered by a number of performances. The drilling settings were optimised using the Taguchi method. Tool diameter. The ideal drilling settings for generating a high value of s/n ratios for the surface roughness of the hole were discovered to be a drilling depth of 8 mm, a rotation speed of 1400 rev/min, and a feed rate of 0.10 mm/rev. While it was discovered that the ideal drilling parameters for creating high-value s/n ratios for both tool wear and material removal rate were a tool diameter of 6 mm, a rotation speed of 600 rev/min, and a feed rate of 0.10 mm/rev [52].

2.1. AIM OF THE STUDY

AISI 304 stainless steel is used in a wide range of crucial applications, including the production of tools and die-making. In this research, two distinct Taguchi models will be created utilizing two alternative designs in compliance with set machining

parameters. The first model includes close parameters, and the second model includes the far parameters. These two models were created to study the effects of speed and feed rate on surface roughness and cutting forces when drilling AISI 304 Stainless Steel with carbide drill bits. After that, the study will concentrate on how machining parameters affect cutting force and surface integrity, and chip formation The four primary goals of this study are to contribute experimental data on Inconel AISI 304 Stainless Steel drilling to the literature and allow for comparison with previous researchers that investigate machining modeling.

- ✓ AISI 304 Stainless Steel will be used to examine how speed and feed rate affect surface roughness and cutting forces for two different Taguchi models.
- ✓ The experiments were performed using different cutting depth phases to study the cutting forces by the CNC milling machine with a carbide twist drill and a carbide twist drill.
- ✓ Study the chip morphology of each experiment.
- ✓ Analysis of variance (ANOVA), regression analysis, and optimization were applied, and results were compared by Minitab software.

PART 3

METHODOLOGY

3.1. INTRODUCTION

In general, choosing the right machining conditions is crucial when cutting metal. The operator's experience is crucial in these situations, but even a skilled operator finds it challenging to maximize these values throughout each machining process.. In this part, the work plan and the experimental Design, setup, and Required Equipment of this study will be clarified in detail.

3.2. WORK PLAN

In order to achieve the best results in this study, the following work plan as shown in Figure 3.1 will be considered:

- ✓ Two different Taguchi models: the first one contains close parameter levels and the second contains far parameter levels.
- ✓ Selecting the material of the sample, machine type, and the necessary measuring devices.
- ✓ Select the cutting tool.
- ✓ Calculate the feed and speed of cutting by the Mastercam software or according to the manufacturer's calculations of the tool.
- ✓ Use the software Solidworks to create the example.
- ✓ Minitab software created an experimental design.
- ✓ Conduct the experiments using a CNC milling machine.
- ✓ Results evaluation Ra, tool forces, machining time, and chip type.
- ✓ Analysis results by Minitab software, Optimization (Signal/Noise) Variance analyses, and (ANOVA) Regression analyses

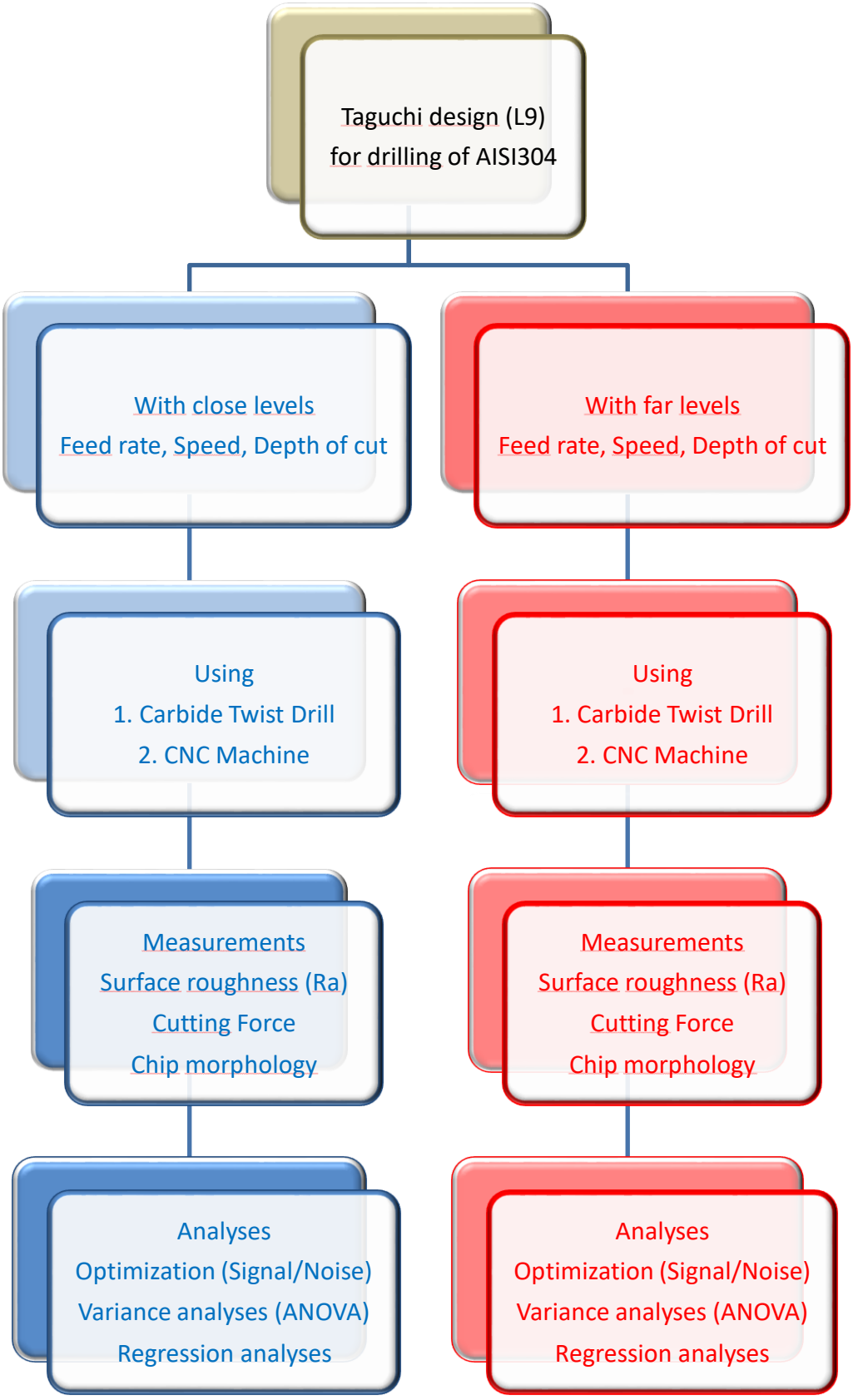

Figure 3.1.Work Plan

3.2. RAW MATERIAL

In this study, the experimental sample is made of AISI 403 stainless steel with dimensions as shown in Figure 3.2. This size is specified to fit with stationary dynamometer equipment that was installed in a CNC milling machine.

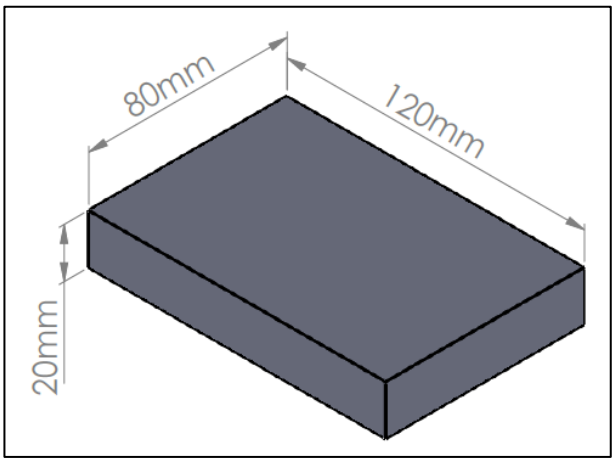

Figure 3.2. Experimental Sam.

3.2.1. Sample Design

The current investigation's workpiece is made of material that measures 120 mm by 80 mm by 20 mm and contains 18 holes that are each 10 mm in diameter, as shown in Figure 3.3.

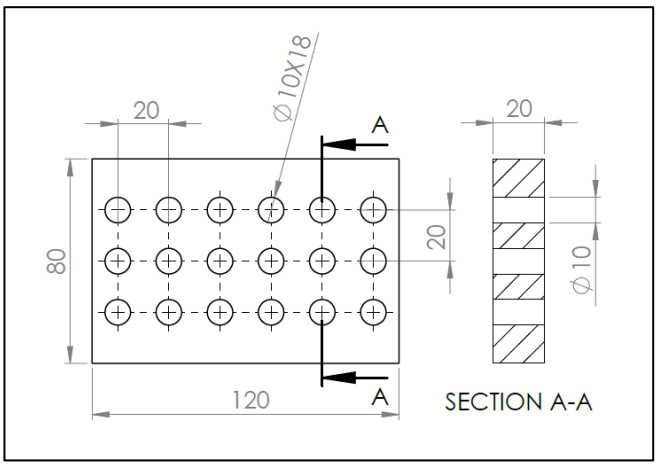

.

Figure 3.3.Workpiece.

3.3. TOOLS

This study used the twist solid carbide drill. The drill diameter is 10 mm and the length is 120 mm as shown in Figure 3.4.

Figure 3.4. The twist solid carbide drill.

3.4. CALCULATION SPEED AND FEED

In order to calculate the appropriate speed and feed rate, in this study, one of the free good websites is considered to provide free information in calculating the speed of cutting and feed rate in milling, lathe, and drilling. Here an application known as Speed Doctor is used as shown in Figure 3.5 [53].

Figure 3.5. Speed Doctor calculates S&F [53].

3.4.1. Calculation Speed and Feed of The First and Second Group

For calculating the cutting feed rate and speed to the first and second groups according to the speed doctor website. As seen in figure 3.6, firstly, the selection of the appropriate setting such as; Units, Application, and Material Group as shown in figure 3.6 (a).

secondly, defined the required raw material (AISI 403) from the list can be seen in figure 3.6 (b). lastly in this part, the required tool application as tool type, the diameter of the drill and number of flutes, RPM and the power limits need to be defined as can be seen in figure 3.6 (c). After that, in the fourth step for calculating the feed rate and the speed of the First Group in the Calculation choose (Longer tool life) for the speed control and (Automatic) for the feed control see figure 3.6 (d). However, for the second group select (Aggressive) for the speed control and (Automatic) for the feed control see figure 3.6 (e). After that the results of the Cutting speed and feed rate for the First Group experiments come to, 640 rpm with 0.17mm/min respectively figure 3.6 (f). Whereas the results of the second group experiments are 1270 rpm and 0.22 mm/min respectively figure 3.6 (g).

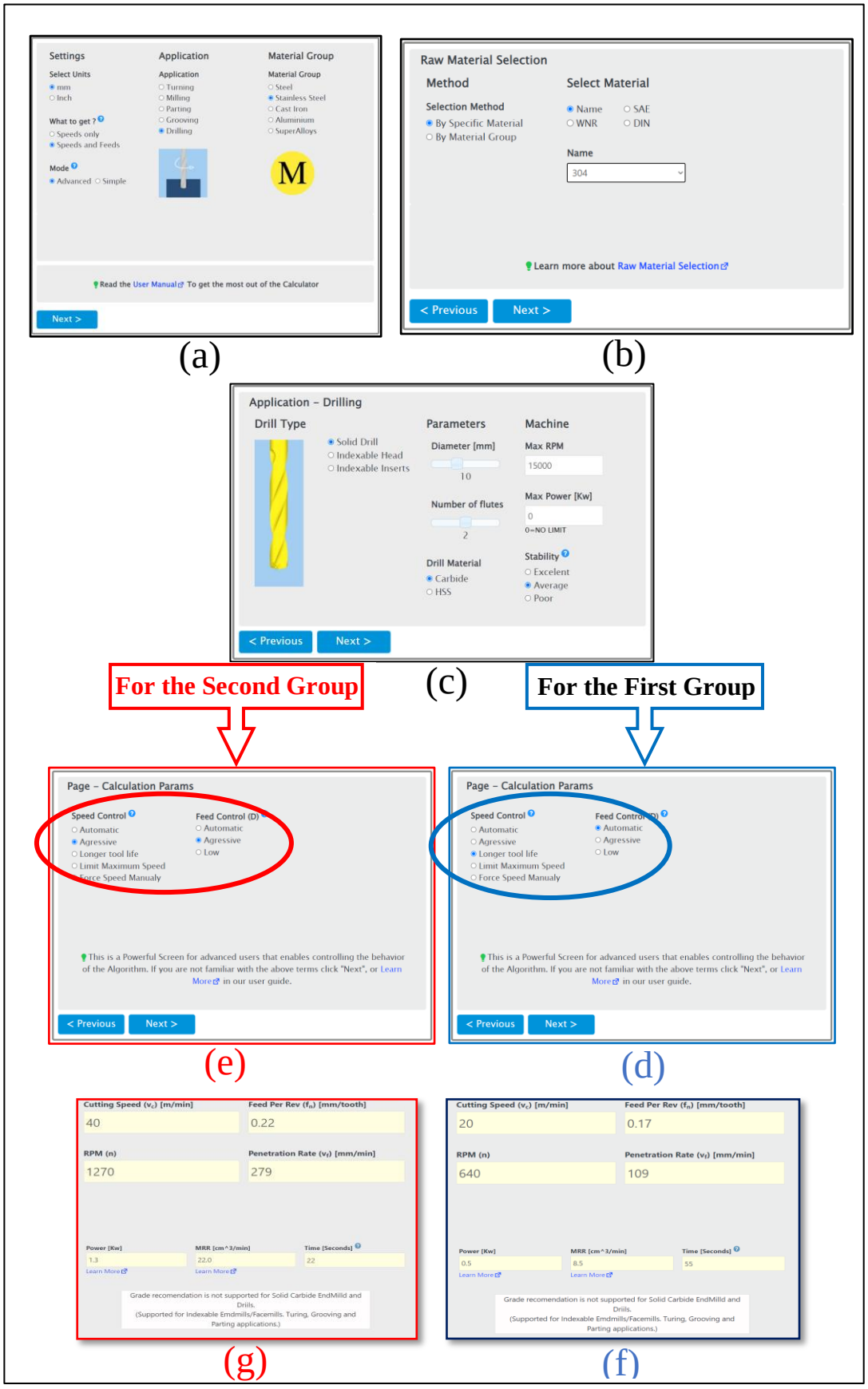

Figure 3.6. Calculate Speed and Feed [53].

3.5. EXPERIMENTAL DESIGN USING TAGUCHI METHOD

The Taguchi method, one of the greatest experimental techniques, is used to calculate the minimum number of tests that must be performed while remaining within the permissible range of levels and parameters in order to reduce expenses.

In this study, the level disparities will be maintained in the first experimental group design at a minimum level of around (20%) and in the second experimental group design at a maximum level of around (40%). Therefore, using Taguchi design and the Minitab program, the results of the trials for the first and second groups were obtained, tables 3.1 and 3.2, respectively, showed the parameters.

Table 3.1. The first group factor design.

Close levels (20%)			
Parameters	Level (1)	Level (2)	Level (3)
Feed rate (mm/min)	0.13	0.17	0.2
Cutting Speed (rpm)	512	640	768
Step increment of Depth of cut 20 (mm)	5	8	10

Table 3.2. The second group factor design.

Close levels (20%)			
Parameters	Level (1)	Level (2)	Level (3)
Feed rate (mm/min)	0.13	0.22	0.3
Cutting Speed (rpm)	774	1270	1766
Step increment of Depth of cut 20 (mm)	5	8	10

3.5.1. Experimental Design of the first group

Table 3.3 displays the first group's experimental settings according to the Taguchi method design.

Table 3.3. Parameters of the first group.

Exp. No.	Parameters		
	Feed rate mm/min	Speed rpm	Step increment mm
1	0.13	512	5
2	0.13	640	8
3	0.13	768	10
4	0.17	512	8
5	0.17	640	10
6	0.17	768	5
7	0.2	512	10
8	0.2	640	5
9	0.2	768	8

3.5.2. Experimental Design of the second group

Table 3.4 displays the second group's experimental settings according to the Taguchi method design.

Table 3.4. Parameters of the second group.

Exp. No.	Parameters		
	Feed rate mm/min	Speed rpm	Step increment mm
1	0.13	774	5
2	0.13	1270	8
3	0.13	1766	10
4	0.22	774	8
5	0.22	1270	10
6	0.22	1766	5
7	0.3	774	10
8	0.3	1270	5
9	0.3	1766	8

3.6. EXPERIMENTAL WORKS

All experimental work were on the CNC milling machine, Falco, HAAS VF-2SS which is shown in Figure 3.7, with a specification listed in Table 3.5. A Solid carbide drill tool with a diameter of 10 mm is used for this experimental work, see Figure 3.8, and the workpiece material is chosen from the stainless steel 403.

Table 3.5. CNC Machine specifications [54].

MOVEMENTS	**METRIC**	**SPINDLE**	**METRIC**
X-axis	762 mm	Max. Strength	22.4 kW
Y Axis	406 mm	Max Speed	12000 rpm
Z Axis	508 mm	Maximum Torque	122.0 Nm @ 2000 rpm
Spindle End Norm to Table (~max.)	610 mm	Bearing Lubrication	Air / Oil Injection
Spindle End Norm to Table (~min.)	102 mm	Cooling	Liquid Cooled
TABLE	METRIC	FEEDRATES	METRIC
Length	914 mm	Maximum Cut off	21.2 m/min
Width	356 mm	Speeds in X	35.6 m/min
T Channel Width	15.90 mm to 16.00 mm	Speeds in Y	35.6 m/min
T-Channel Center Distance	125 mm	Speeds in Z	35.6 m/min
Number of Standard T Channels	3		
Max. Weight (evenly distributed)	680 kg		
ELECTRICALSPECIFICATION	METRIC	AXIS MOTORS	METRIC
Spindle Speed	12000 rpm	Max. Thrust X	8874 N
Drive System	Inline Direct Drive	Max. Thrust Y	8874 N
Spindle Power	22.4 kW	Max. Thrust Z	13723 N
Input AC Voltage (3 Phase) -Low	220VAC		
Full Load Amps (Phase 3) – Low	70 A		
Input AC Voltage (3 Phase) - High*	440 VAC		
Full Load Amps (3 Phase) -High*	35 A		
DIMENSIONS – SHIPPING		METRIC	
Domestic Pallet		257 cm x 251 cm x 257 cm	
Export Pallet		249 cm x 232 cm x 254 cm	
Weight		3539.0 kg	

Figure 3.7. HAAS VF-2SS milling machine.

Figure 3.8. Experimental Works.

In this research work, a stationary Dynamometer shown in Figure 3.9 is used to measure cutting forces. The dynamometer is firmly mounted on the table of the CNC milling machine while the workpiece is clamped on the top of the Dynamometer surface. In addition, in this experiment work a Multichannel Charge Amplifier shown in Figure 3.10 is used to convert the high-impedance charge input into a usable output voltage.

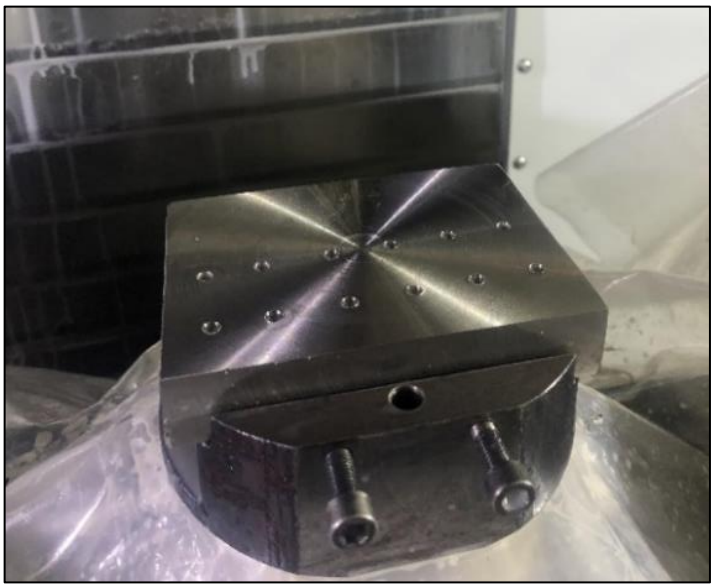

.

Figure 3.9. Stationary dynamometer.

Figure 3.10. Multichannel charge amplifier.

3.7. SURFACE ROUGHNESS MEASUREMENT

Surface Roughness Measuring Device SJ-410 that shown in Figure 3.11 is used in this work, it provides a wide measuring range and different roughness parameters. It has a maximum range of 800 μm (±400 μm) and can display different roughness parameters. In addition, giving measurement results in accordance with different roughness standards [55].

Figure 3.11. Surface Roughness Measuring Device SJ-410 [55].

3.8. USB MIKROSKOP

In order to obtain microscopic images for the chip was used 1000x2 MP Digital Stand 8 Led USB Microscope was as shown in figure 3.12.

Figure 3.12. USB Microscope [56].

PART 4

RESULTS AND DISCUSSION

4.1. INFLUENCE OF MACHINING PARAMETERS ON CHIP FORMATION DURING DRILLING OPERATION

In this stage, the impact of the machining parameters on the formed chips for the experiments of the first and second groups will be examined using formed chip samples collected during drilling operations.
Based on the chip formations acquired from this experiment, the continuous chips are categorized into spiral and string chips.

- ✓ spiral chips
  - o tight helix-
  - o loose helix chips.
- ✓ string chips.
  - o short ribbon chips.
  - o long ribbon chips.

4.1.1. Explanation of experiments of first group chip

Results of the first group's drilling experiments demonstrated that chips formed with a significant thickness of about 4 mm are broken at 768 rpm with 0.13 and 0.17 mm/min feed rates, this is clearly shown in both experiments 4 and 7. (Figure 4.1). But when lowered the speed to 512 rpm with a feed rate of 0.13 mm/min in experiment number 2 newly formed chips are short ribbon chips and spiral with loose helix chips, while when increase the feed rate to 0.17 mm/min, the formed chips are spiral and short serrated ribbon chips.

In experimental number 7, by using a cutting speed of 768 rpm with a feed rate of 0.17 mm/min, the created chips were tight helix spiral chips, short ribbon chips, and long serrated ribbon. A variety of chip sizes typically implies that the flank wear on both sides and the two cutting-edge angles and lengths are not symmetrical.

With a feed rate of 0.13 mm/min and two rates of cutting speeds of 512 and 768 rpm, the chips formed a spiral with helix chips. On the other hand, the chips in trials 8 and 9 with increasing the feeding rate to 0.2 min/mm with 640 and 768 rpm were thick and sharp chips, which typically resulted in damage to the cutting tool and the machine. In this series of experiments, drilling AISI 304 generally produced helix chip shapes when cutting speed and feed rates were low. On the other side, drilling with faster cutting speeds and feed rates produced loose string chips, which were not the desirable chip shapes. The chip morphologies from the first group's nine drilling tests are shown in Figure 4.1.

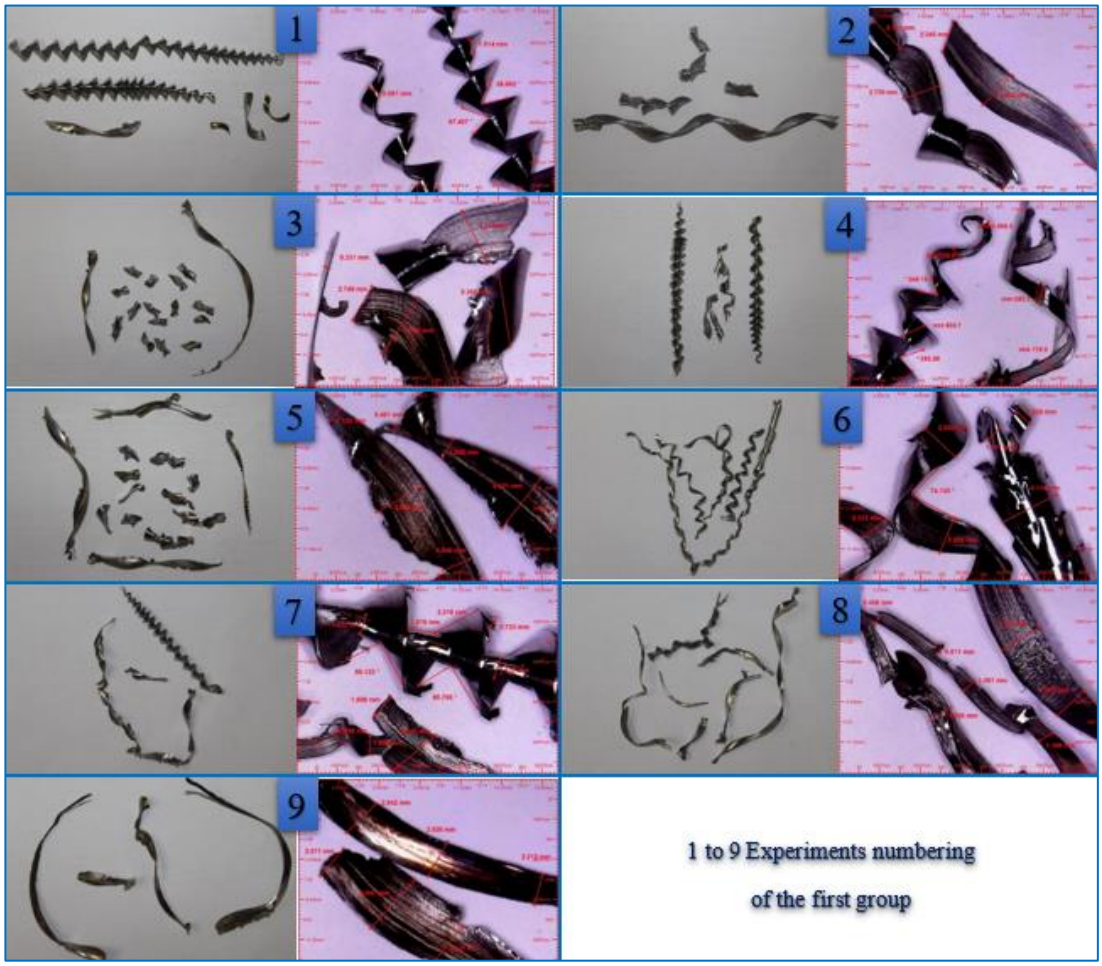

Figure 4.1. Chip of the First Group.

4.1.2. Explanation of experiments of second group chip

In the second set of drilling experiments, short ribbon chips with a spiral and a wire thickness of 2 mm were created at 774 and 1270 rpm with 0.13 and 0.22 mm/min feed rates. However, in experiments 4 and 7, the feeding rate was increased to 0.22 and 0.3 mm/min, respectively, while the cutting speed remained at 774 rpm. When using a cutting speed of 1270 rpm and a feed rate of 0.13 mm/min, the results were exceptionally lengthy and continuous chips. Chips were developed when the helix was free, and spiral chips and while short, serrated ribbon chips were developed when the feed rate was 0.17 mm/min.

Only in experiment number 5 when the cutting speed was 1270 rpm with a feeding rate of 0.22 mm/min the results were almost the same; additionally, loose string chips were in most experiments with higher cutting speeds and feed rates. In general, experiments numbers 1 and 7 with lower cutting speeds of 774 rpm and feed rates of 0.13 and 0.3 mm/min, resulted in the creation of helix chips. The chips from the second group were shown in Figure 4.2.

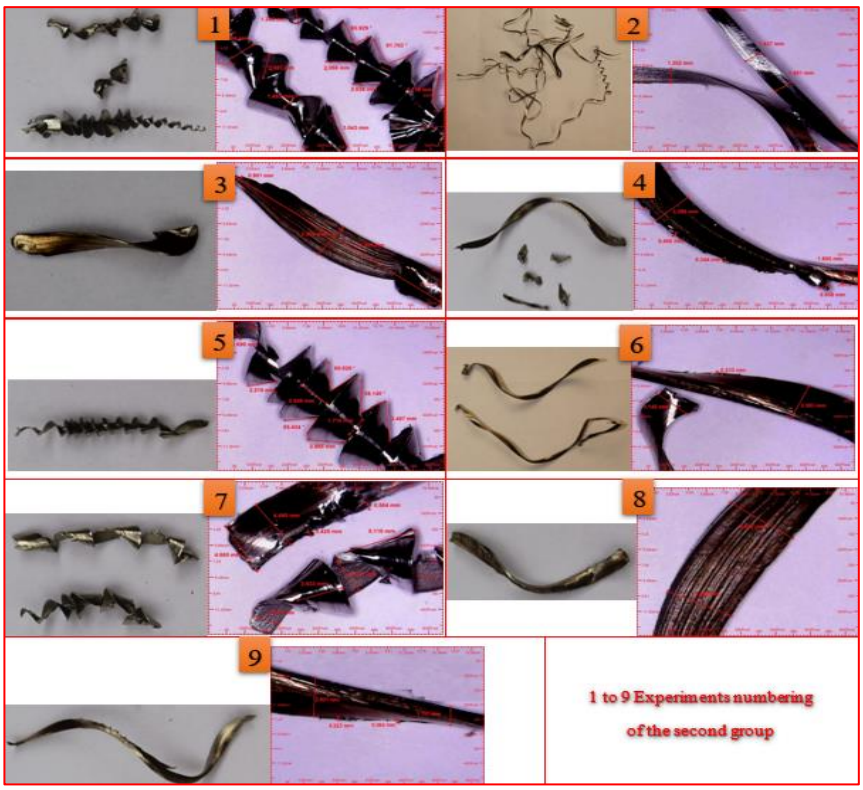

Figure 4.2. Chip of the Second Group.

4.1.3. Comparison between first and second group chips

The best chips from the first experimental group were produced in experiments 1, 4, and 7 with 512 rpm cutting speed with various feed rates, as shown in Figure 4.3. While the best chips from the second experimental group were produced in experiments 1 and 5 with 774 and 1270 rpm cutting speeds and feed rates of 0.13 and 0.22 mm/min, respectively, as shown in Figure 4.4.

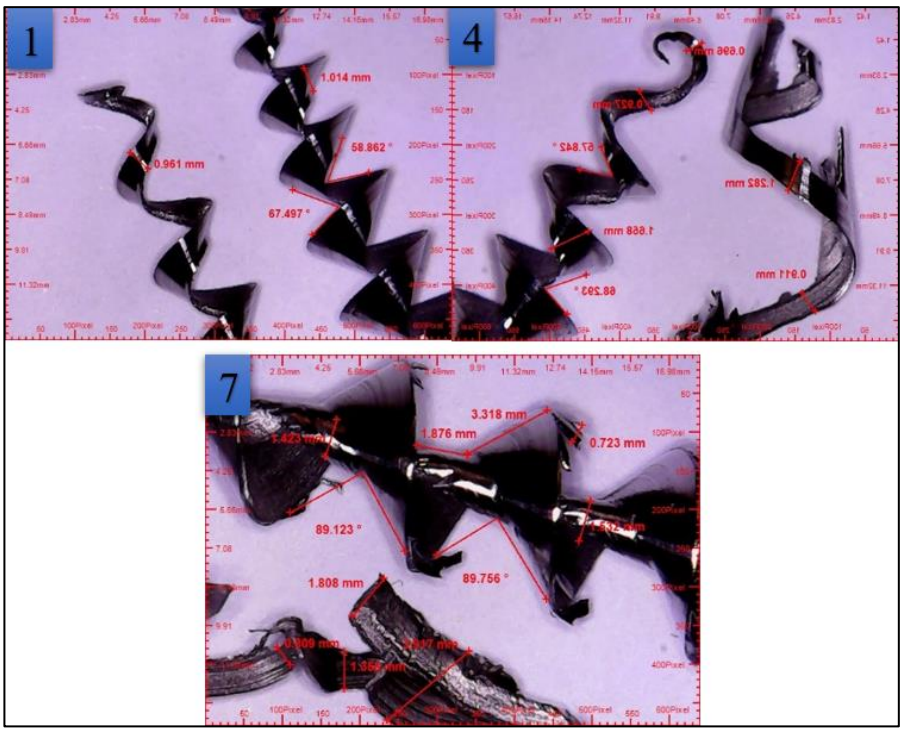

Figure 4.3. The chips of experiments number 1,4 and 7 (first group).

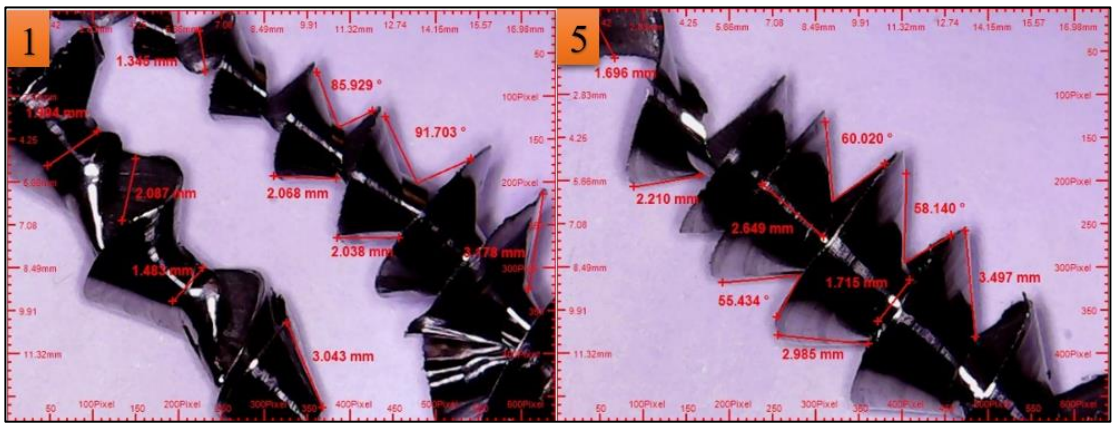

Figure 4.4. The chips of experiments number 1and 5 (second group).

4.3. SURFACE ROUGHNESS MEASUREMENTS (Ra)

Figure 4.5 shows a typical surface roughness profile. Ra, P, and Ry, which stand for maximum peak-to-valley roughness and root mean square roughness, respectively, reflect average surface roughness (RMS). This area is also referred to as the space between the roughness profile and its mean line. The equation can also be used to integrate the absolute value of the roughness profile height over the sampling length to determine the average surface roughness Ra (4.1).

$$R_a = \frac{1}{l}\int y(x)dx \tag{4.1}$$

- ✓ The average surface roughness is known as Ra.
- ✓ The sample length is L.
- ✓ The coordinate of the profile curve is x.

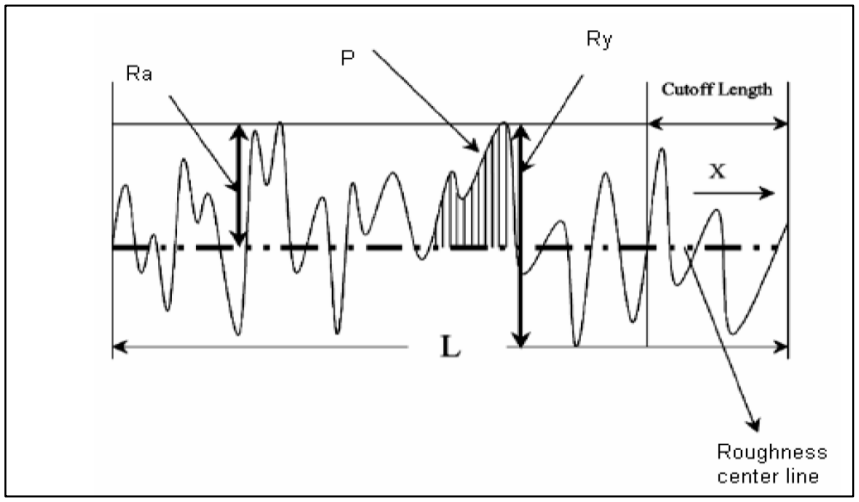

Figure 4.5. Surface Roughness Profile [57].

Using a surface roughness profilometer from the Mitutoyo surfaces SJ-410 series, the surface roughness values of the holes under each machining condition were evaluated, as illustrated in Figure 3.10. The average value of four measurements from each quarter in each hole was used to calculate the average surface roughness of each hole, as illustrated in Figure 4.6.

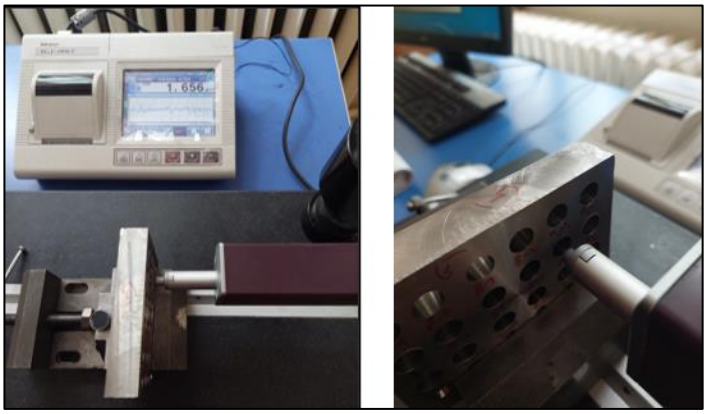

Figure 4.6. Surface Roughness Measure

4.3.1. Results of Surface Roughness Ra of First Group

According to Figure 4.7, four points of surface roughness (Ra) were measured in each hole for every experiment. For the first group experiments, the average was determined and noted, as shown in Table 4.1.

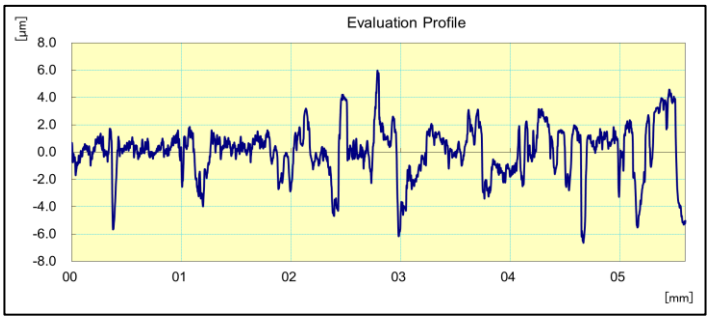

Figure 4.7. Ra of the First Group.

Table 4.1. Ra Average of the first group.

Exp. No.	Feed rate mm/min	Speed rpm	Step increment mm	Ra µm
1	0.13	512	5	2.385
2	0.13	640	8	1.919
3	0.13	768	10	2.348
4	0.17	512	8	1.297
5	0.17	640	10	1.553
6	0.17	768	5	1.870
7	0.2	512	10	0.841
8	0.2	640	5	1.607
9	0.2	768	8	1.591

4.3.2. Results of Surface Roughness Ra of Second Group

In the second group experiments, four points of surface roughness (Ra) were measured in all holes for all experiment values. Also, the average was calculated and recorded for the first group experiments as shown in Figure 4.8. and Table 4.2.

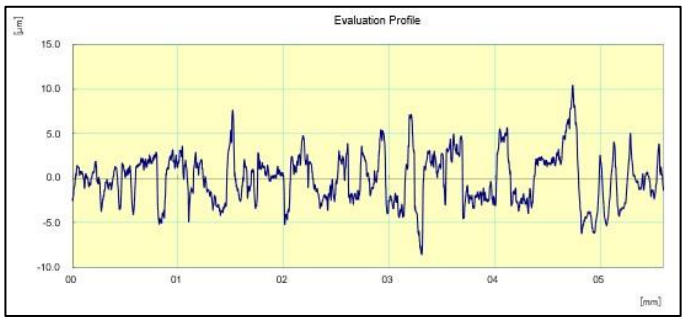

Figure 4.8. Ra of the second Group.

Table 4.2. Ra average results of second group.

Exp. No.	Feed rate mm/min	Speed rpm	Step increment mm	Ra µm
1	0.13	774	5	1.303
2	0.13	1270	8	2.543
3	0.13	1766	10	1.946
4	0.22	774	8	2.093
5	0.22	1270	10	1.522
6	0.22	1766	5	1.599
7	0.3	774	10	1.070
8	0.3	1270	5	1.280
9	0.3	1766	8	1.880

4.3.3. Comparison Between Ra Results of First and Second Group

Figure 4.9 displays the first and second group's surface roughness "Ra" used in this study. The "Ra" values decreased in experiment number 7 in both groups when the cutting speed was 512 rpm with the feed rate of 0.2 mm/min. in the first group and the cutting speed was 774 rpm with a feed rate of 0.3 mm/min, this led to satisfied results of "Ra". However, unrealistic results were obtained in experiment number 5 in both groups showed nearly the same "Ra" values when using the cutting speed of 640 and 1270 rpm with the feed rate of 0.17 and 0.22. While experiment number 2 in the

first group and experiment number 1 in the second group produced the greatest value for Ra results.

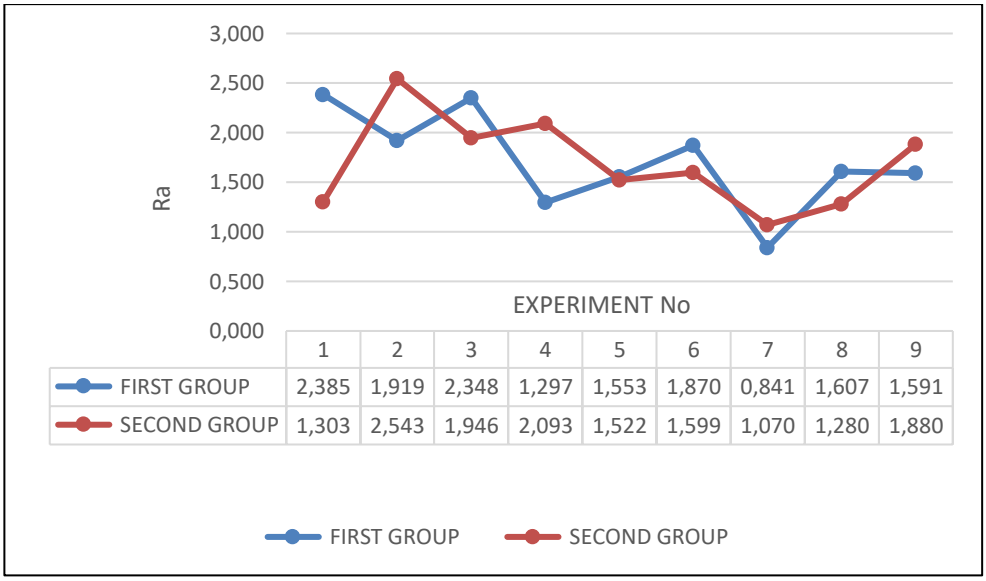

Figure 4.9. Comparison Between Ra of the First And Second Group.

4.4. TOOL FORCE

The cutting forces are extremely challenging to model and forecast. The ability to predict cutting forces enables users to produce high-quality parts more quickly without compromising tool life. Two distinct groups of drilling experiments were performed in the drilling machines at various feed rates and speeds. Different tool force settings were used in each experiment for the two groups.

4.4.1. Tool Force of The First Group

A typical drilling force-time graph is shown in Figure 4.10. The force-mean of the first group experiment is displayed in Table 4.3. Additionally, as seen in the same table, drilling-induced thrust force increased with higher cutting speed and feed values, with experiment number 9's cutting parameters of 0.2 mm/min feed rate and 768 rpm producing the highest values for Force-Mean and Moment-Mean, respectively, of 2178 N and 690.2 Ncm.

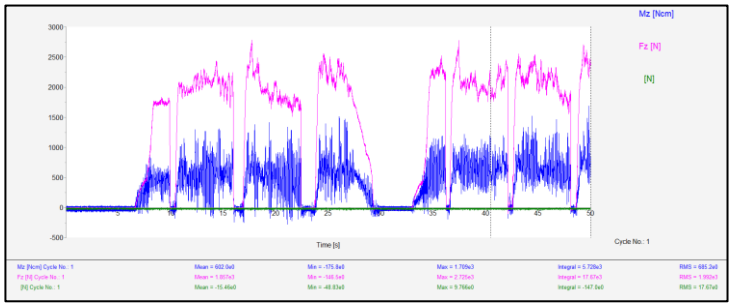

Figure 4.10. Force-Time of the first group

Table 4.3. Main Force Average of The First Group

Exp. No.	Feed rate mm/min	Speed rpm	Step increment mm	Force-Mean (N)	Moment-Mean (Ncm)
1	0.13	512	5	1346	413.9
2	0.13	640	8	1367	534.4
3	0.13	768	10	1593	622.6
4	0.17	512	8	1654	430.9
5	0.17	640	10	1690	547.6
6	0.17	768	5	2117	682.1
7	0.2	512	10	1926	519.4
8	0.2	640	5	1799	563.9
9	0.2	768	8	2178	690.2

4.4.2. Tool Force of the Second Group

One of the tests in the second group experiment is illustrated by the average main force of the second group graph in Figure 4.11. The Force-Mean and Moment-Mean for each of the second group trials are likewise included in Table 4.4. Additionally, as the cutting speed is increased and the feeding rate is maintained, the Force-Mean and Moment-Mean in testing Nos. 3, 6, and 9 decrease slightly.

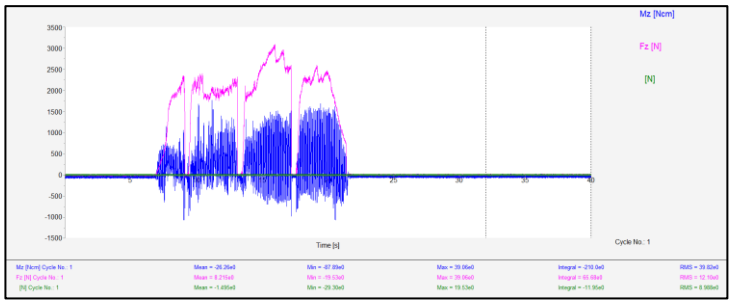

Figure 4.11. Force-Time of the Second Group.

Table 4.4. Main Force Average of the Second Group

Exp. No.	Feed rate mm/min	Speed rpm	Step increment mm	Force-Mean (N)	Moment-Mean (Ncm)
1	0.13	774	5	1612	487.5
2	0.13	1270	8	1604	698.3
3	0.13	1766	10	1852	850.3
4	0.22	774	8	2010.2	727.9
5	0.22	1270	10	2230	789.3
6	0.22	1766	5	2567	839.5
7	0.3	774	10	2713	886.5
8	0.3	1270	5	2890	970.3
9	0.3	1766	8	2910	1230.5

4.4.3. Comparison Between the Average Main Force of the First and Second Group Experiments

The experimental results for the first and second groups in Figure 4.12 demonstrate that the force (Fz and Mz) increases as the feed rate increases because the cutting tool is attempting to remove more material. The material removal rate (MRR) rises with the increased feed rate. Furthermore, it is clear from the first three experiments that the lowest values for both groups were quite near to each other. For instance, in the first experiment, Fz 1612 and 1346 N were closely followed by Mz 413.9 and 487.5 MN of the first and second groups, respectively. However, when examining all of the first group's experiments, similar results were obtained, with Fz ranging between 1000 and 2200 N and Mz ranging between 400 and 700 Ncm. However, it was noted that the second group increased its force Mz and Fm after the sixth experiment, peaking almost at about 3000 N for Fz and 1250 Ncm for Mz. Since the feeding rate was 0.13 mm/min in both groups, the result was nearly identical to experiment number 1. This indicates that the feeding rate had a significant impact on the force in general.

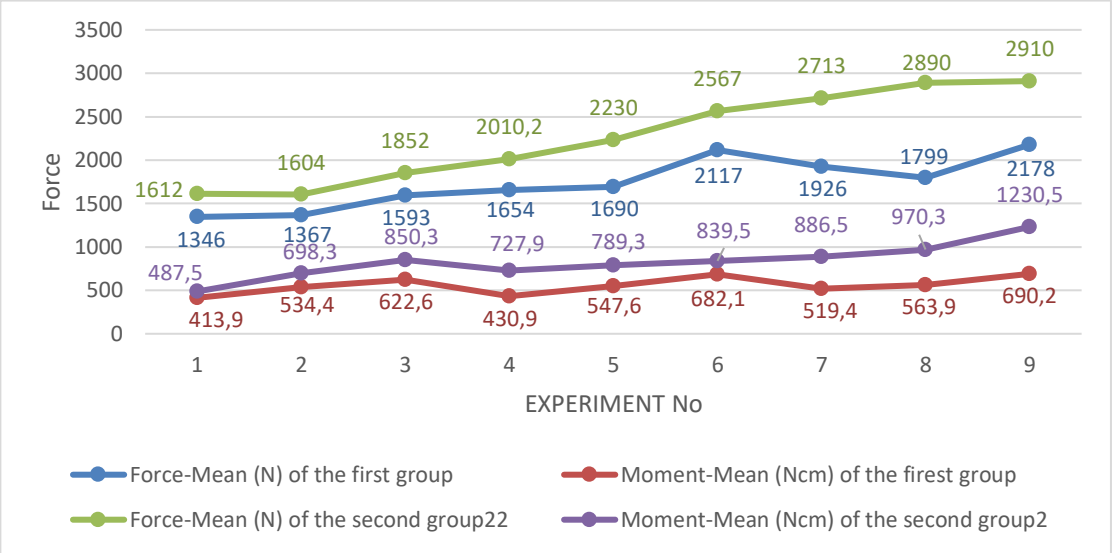

Figure 4.12. Comparison Between The Average Main Force.

4.5. ANALYSIS RESULTS USING MINITAB SOFTWARE

In this study, the results for each experiment in the first and second groups were analyzed using Minitab software. The analysis was performed using the next three steps.

- ✓ Analysis of Variance (ANOVA).
- ✓ Taguchi analysis design.
- ✓ 3D surface plot.

4.5.1. Analysis Variance Using ANOVA

The statistical analysis method known as analysis of variance (ANOVA) divides the observed aggregate variability within a data set into two portions: random factors and systematic factors. In contrast to random effects, systematic factors have a statistical impact on the supplied data set. The ANOVA test is used by analysts to evaluate the impact of independent factors on the dependent variable in a regression analysis [58]. The Minitab program was used in this research to get the ANOVA test results. The ANOVA test is a helpful tool for establishing whether the results of an experiment are significant since it can show the impact of variables like cutting speed, feed rate, and steps on Ra, Fz, and Fm of the experimental outcomes.

4.5.2. Ra Results Analysis of First Group Using ANOVA

Utilizing the statistical application Minitab-17, an ANOVA is produced. Understanding the effect of the first group's cutting speed, feed rate, and steps on the "Ra" result depends on understanding the "Ra" analysis of variance significant analysis, which is shown in Table 4.5. The feed rate, cutting speed, and 64.48%, 14.54%, and 13.82%, respectively, have an impact on the "Ra" values. The main effect comes from the feed rate. Table 0.5 Analysis of Variance (ANOVA) for Ra's the First Group. Additionally, Table 4.6. displayed the first group's Model Summary of Ra results analysis.

Table 4.5. Ra Results Analysis of First Group Using ANOVA.

Source	DF	Adj SS	Adj MS	F-Value	P-Value	Contribution (%)
Feed rate (mm/min)	2	1,2249	0,61245	8,67	0,103	64.48
Speed (rpm)	2	0,2773	0,13866	1,96	0,338	14.54
Step (mm)	2	0,2635	0,13176	1,86	0,349	13.82
Error	2	0,1413	0,07066			
Total	8	1,9070				

Table 4.6. Ra Model Summary of First Group.

S	R-sq	R-sq(adj)	R-sq(pred)
0.208650	88.59%	81.74%	52.21%

The following equation forms (4.2) a regression equation model for minimising the surface roughness value, Ra, Feed rate, Speed and Step.

Ra-Avg = 3.346 - 12.64 Feed rate + 0.001674 Speed - 0.0780 Step (4.2)

4.5.3. Ra Results Analysis of Second Group Using ANOVA

As indicated in Table 4.7, the effects of the feed rate, cutting speed, and steps on the Ra values are 24.03%, 10.91%, and 60.92%, respectively, which is crucial for understanding how these elements affect the Ra result for the second group. the steps have the most impact on this group was 60.29%. Also, Table 4.8. showed Model Summary of Ra results analysis of the second group.

Table 4.7. Ra Results Analysis of Second Group Using ANOVA.

Source	DF	Adj SS	Adj MS	F-Value	P-Value	Contribution (%)
Feed rate(mm/min)	2	0,41580	0,20790	5,80	0,147	24.03
Speed (rpm)	2	0,18875	0,09437	2,63	0,275	10.91
Step (mm)	2	1,05409	0,52704	14,70	0,064	60.92
Error	2	0,07172	0,03586			
Total	8	1,73035				

Table 4.8. Ra Model Summary of Second Group.

S	R-sq	R-sq (adj)	R-sq (pred)
0,189369	95,86%	83,42%	16,07%

For minimizing the surface roughness value, Ra, Feed rate, Speed, and Step, use the regression equation model shown in equation (4.3).

Ra = 1,619 - 3,04 Feed rate mm/min + 0,000322 Speed rpm + 0,0423 Step mm (4.3)

4.5.3. Comparison Between First and Second Groups of Ra Results Analysis Using ANOVA

The first and second groups' ANOVA findings are shown in Tables 4.5 and 4.7, respectively. The first group's feed rate had the greatest percentage impact on the Ra results (64.48%), while the second group had the greatest percentage impact on the cutting parameters (60.92%). Ra is least affected by the cutting speed rates of 14.54 and 10.91% in the first and second groups.

4.5.3. Force-mean Analysis of First Group Using ANOVA

Understanding how the cutting parameters affect the Force-mean result for the First group is essential. The influence of the cutting parameters on the Force-mean of the First Group were the feed rate 64.95%, cutting speed 31.77%, and steps 0.1%, respectively. While the effect of the step was only marginal, at 0.1%, as shown in Table 4.9, the feed rate has the greatest influence on this group. Table 4.8. also included an analysis of the first group's Model Summary of Fz results.

Table 4.9. Fz Analysis of First Group Using ANOVA.

Source	DF	Adj SS	Adj MS	F-Value	P-Value	Contribution (%)
Feed rate (mm/min)	2	453311	226655	20,49	0,047	64.95
Speed (rpm)	2	221708	110854	10,02	0,091	31.77
Step (mm)	2	764	382	0,03	0,967	0.10
Error	2	22126	11063			
Total	8	697909				

Table 4.10. Fz Model Summary of First Group.

S	R-sq	R-sq(adj)	R-sq(pred)
143.373	85.27%	76.44%	49.49%

The following equation forms (4.4) a regression equation model for minimising the the Force-mean value, Fz, Feed rate, Speed and Step.

Force-Mean = -317 + 7714 Feed rate + 1.253 Speed - 3.8 Step (4.4)

4.5.4. Force-mean Analysis of Second Group Using ANOVA

The factors that had the greatest influence on the Force-mean of the Second Group were the feed rate (59.95%), cutting speed (23.9%), and steps (9.55%). Even so, the percentage results weren't much different from the first group as shown in Table 4.11, the step's impact was only marginal in this case (9.55%), and the feed rate once again has the biggest impact on this group. Also, Table 4.12. showed Model Summary of Fz results analysis of the second group.

Table 4.11. Fz Analysis of Second Group Using ANOVA.

Source	DF	Adj SS	Adj MS	F-Value	P-Value	Contribution (%)
Feed rate (mm/min)	2	1201242	600621	9,23	0,098	59.95
Speed (rpm)	2	480782	240391	3,70	0,213	23.99
Step (mm)	2	191354	95677	1,47	0,405	9.55
Error	2	130105	65052			
Total	8	2003482				

Table 4.12. Fz Model Summary of Second Group.

S	R-sq	R-sq(adj)	R-sq(pred)
255,054	93,51%	74,02%	0,00%

The following equation forms (4.5) a regression equation model for minimising the Force-mean value, Fz, Feed rate, Speed and Step.

Mean Fz (N) =880 + 4866 Feed rate + 0,261 Speed - 8,2 Step increment (4.5)

4.5.5. Moment-Mean Analysis of First Group Using ANOVA

As indicated in Table 4.13, the effects of cutting speed on the Moment-Mean values was at the biggest value with 87.4%. However. The effect of the feed rate and steps were extremely small less than 10%. Also, Table 4.14. showed Model Summary of Mz results analysis of the first group.

Table 4.13. Mz Analysis of First Group Using ANOVA.

Source	DF	Adj SS	Adj MS	F-Value	P-Value	Contribution (%)
Feed rate (mm/min)	2	6871,0	3435,5	2,77	0,265	9.03
Speed (rpm)	2	66548,7	33274,4	26,85	0,036	87.4
Step (mm)	2	229,4	114,7	0,09	0,915	0.30
Error	2	2478,7	1239,4			
Total	8	76127,8				

Table 4.14. Mz Model Summary of First Group.

S	R-sq	R-sq(adj)	R-sq(pred)
24.4485	96.07%	93.72%	85.44%

The following equation forms (4.6) a regression equation model for minimising the the Force-mean value, Mz, Feed rate, Speed and Step.

Moment-Mean = -142.0 + 953 Feed rate + 0.8212 Speed + 1.79 Step (4.6)

4.5.6. Moment-Mean Analysis of Second Group Using ANOVA

As seen in Table 4.15, the impacts of cutting speed and step on the Moment-Mean values were quite similar. with rough value of 23% figure. However. The feed rate had a 47.47% greater effect on the Moment-Mean than cutting speed and step.

Table 4.15. Mz Analysis of Second Group Using ANOVA.

Source	DF	Adj SS	Adj MS	F-Value	P-Value	Contribution (%)
Feed rate (mm/min)	2	174354	87177	7,70	0,115	47.47
Speed (rpm)	2	84837	42419	3,75	0,211	23.10
Step (mm)	2	85478	42739	3,78	0,209	23.27
Error	2	22642	11321			
Total	8	367312				

Table 4.16. Mz Model Summary of Second Group.

S	R-sq	R-sq(adj)	R-sq(pred)
106,401	93,84%	75,34%	0,00%

The following equation forms (4.7) a regression equation model for minimising the Moment-Mean value, Mz, Feed rate, Speed and Step.

Mean Mz (Ncm)=-241 + 2002 Feed rate + 0,2392 Speed + 47,3 Step increment (4.7)

4.5.7. Comparison Between First and Second Groups of Force-mean and Moment-Mean Results Analysis Using ANOVA

The outcomes of the analysis of the Force-mean and Moment-mean were done using ANOVA. The feed rate had the greatest influence on Force-mean between 65% and 60% in both the first and second groups' tests. However, the moment mean was used for the cutting speed and feed rate, which were 47% and 87.4%, respectively. However, with an effective ratio that varied only between 0.1% and 23%, the steep's impact on Force-mean and Moment-mean in both groups was the least significant of all the cutting factors.

4.6. TAGUCHI METHOD ANALYSIS

A factor's significant level as it relates to a given performance parameter is determined by the Taguchi method analysis. Additionally, many variables can be simultaneously optimized. and as a result, fewer experimental trials can yield more information This can provide solid design solutions and considerably enhance quality.

4.6.1. Ra Analysis of First Group Using Taguchi Method

Taguchi analysis is shown in Figure 4.13 (a) and (b), displaying the Main Effects. Ra-Avg and SN plot. The relationship between the three first group experiment parameters, feed rate, cutting speed, and step with the Ra average outcomes of the first group is expressed as a ratio. The best results of cutting speed were found at 512 rpm, feed rate at 0.2 mm/min, and step at 10mm.

Residual plot for Ra-Avg of the first group in Figure 4.14. The typical Probability Plot displays the individual value deviation from the equation for the regression model. The low deviation is indicated by closely spaced spots around the line.

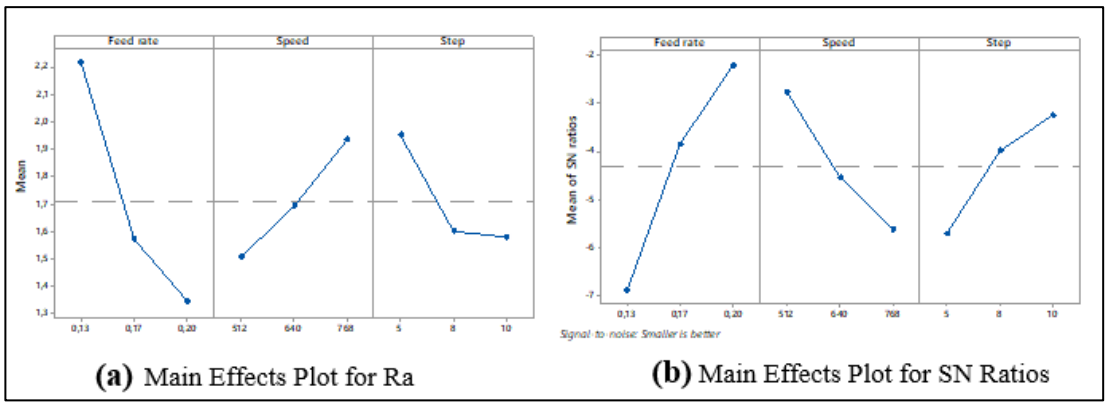

Figure 4.13. Main Effects Plot for Ra-Avg and SN Ratios of The First Group.

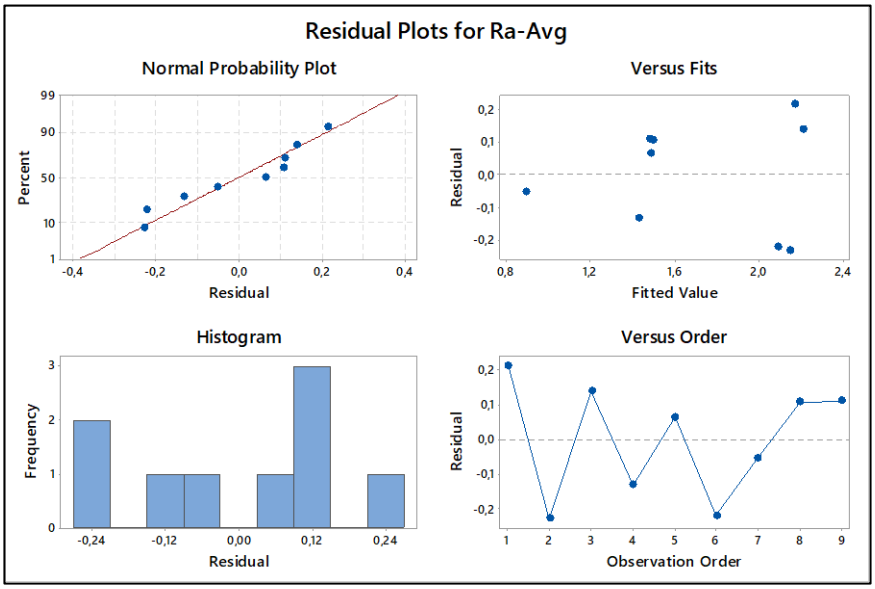

Figure 4.14. Residual plots for Ra-Avg of the first group.

4.6.2. Ra Analysis of Second Group Using Taguchi Method

From Taguchi analysis in figure 4.15 (a) and (b) respectively, the relationship between Ra average results and the three factors (the feed rate, the cuttings speed, and the step) for the second group (0.3 mm/min, 774 rpm, and 5 mm) are the identical respectively. Figure 4.16 shows the Residual plot for the Ra-Avg of the Second group, the results were similar to those of the first group. When compared to the regression model equation, the normal probability plot displays the individual values' deviance. Low deviation can be seen for spots that are closely spaced from the line.

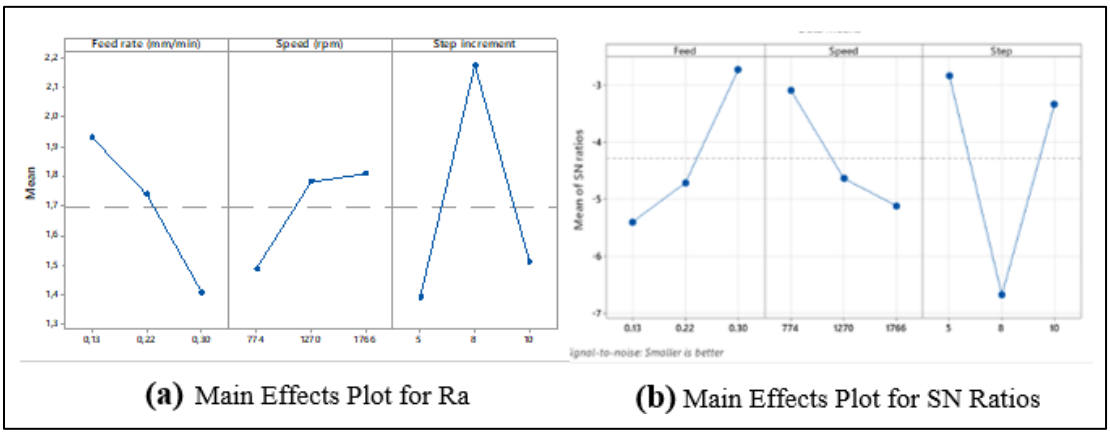

Figure 4.15. Second group main effects for Ra-Avg and SN ratios.

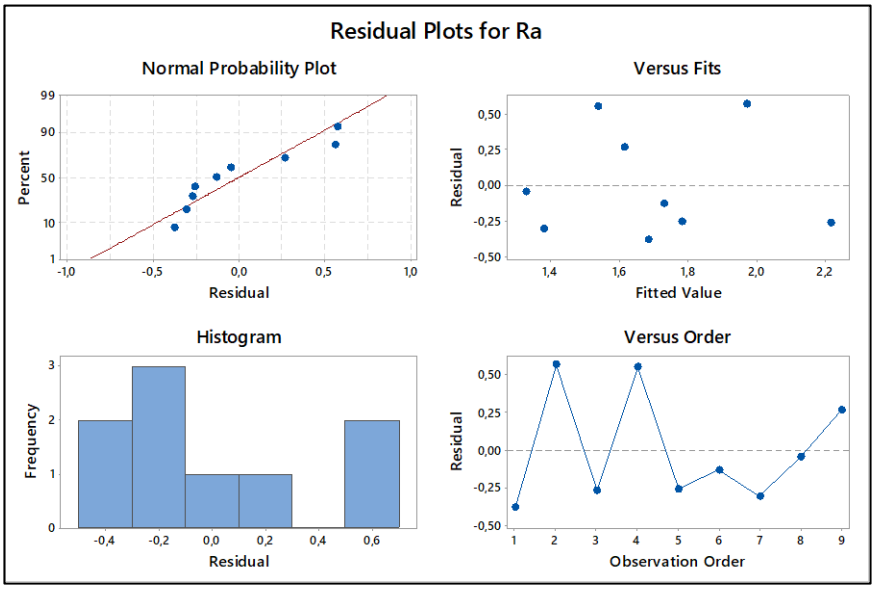

Figure 4.16. Residual plots for Ra of The Second Group.

4.6.3. Comparison Between Ra Taguchi Analysis of First and Second Group

According to the results obtained from Ra Taguchi's analysis of the first and second groups, it was noted that the best results were with the highest feeding rate and the lowest speed for the two groups. The best outcome, however, was for the first group with the highest step, as opposed to the second group with the lowest step.

4.6.4. Force-mean Analysis of First Group Using Taguchi Method

The relationship between the Force-mean findings of the First Group and the three parameters of feed rate, cutting speed, and step for the first group experiments is shown in Figure 4.17 (a) and (b) respectively, which was obtained through Taguchi analysis. It is clearly shown that the optimal values of cutting speed, feed rate, and step are 0.2 mm/min, 670 rpm and 10 mm respectively. Residual plot for Force-mean of the first group in Figure 4.18. The typical Probability Plot displays the individual value deviation from the equation for the regression model. Low deviation can be seen for spots that are closely spaced from the line.

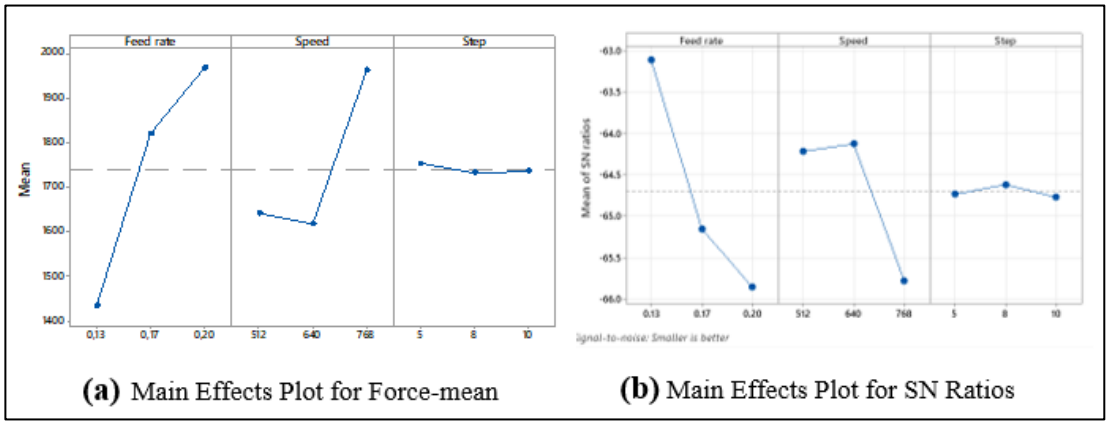

Figure 4.17. Main Effects Plot for Force-mean and SN Ratios of The First Group.

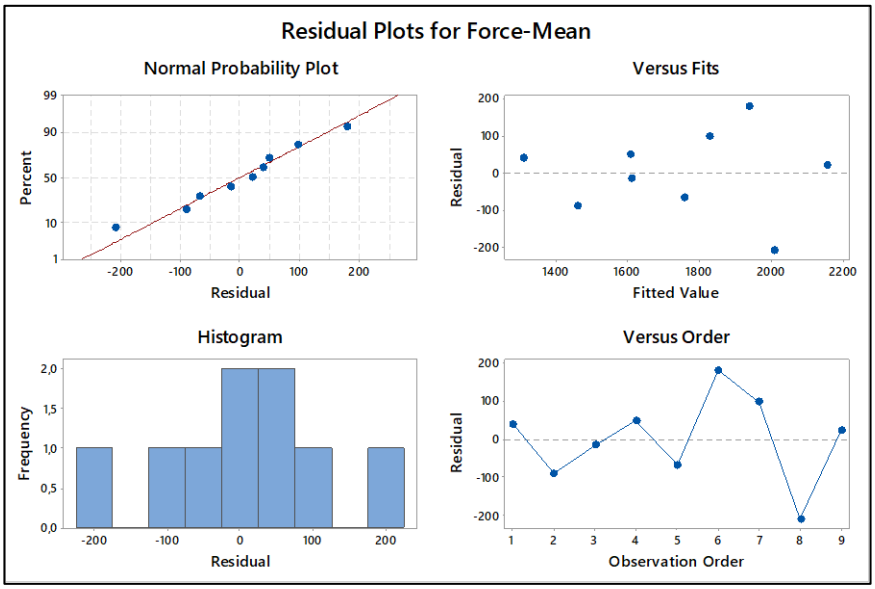

Figure 4.18. Residual plots for Force-mean of The First Group.

4.6.5. Force-mean Analysis of Second Group Using Taguchi Method

Figure 4.19 (a) and (b) show the Force-mean findings of the second group and the three parameters of feed rate, cutting speed, and step. In (a) and (b) graphs from Taguchi analysis, the optimal values of cutting speed, feed rate, and step are 0.3 mm/min, 1270 rpm, and 10 mm respectively. Figure 4.20 shows the Residual plot for the Force-mean of the Second group, it was a small difference as some results diverged obtained from those of the first group it was clearly seen in the sixth, seventh and last experiments. but, In the rest of the experiments, in line with the equation for the

regression model, the typical Probability Plot displays the individual value's deviation. Low deviation can be seen at closely spaced places around the line.

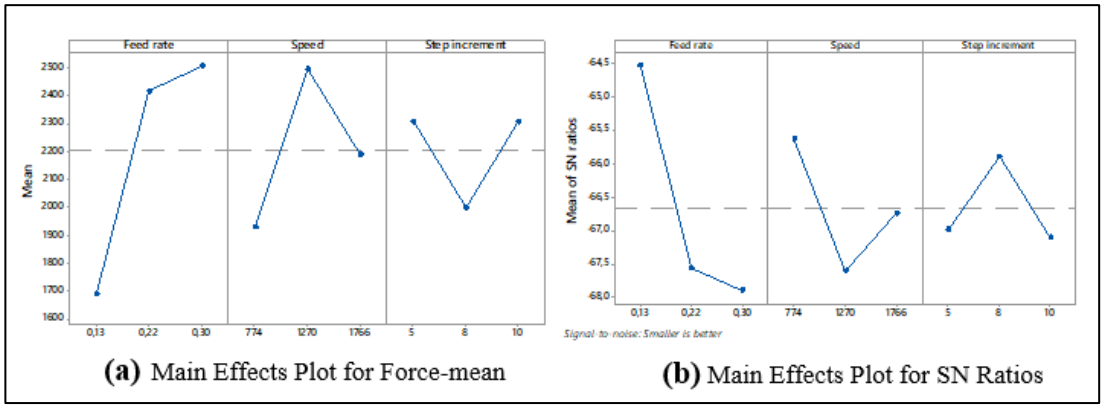

Figure 4.19. Main Effects Plot for Force-mean and SN Ratios of The Second Group.

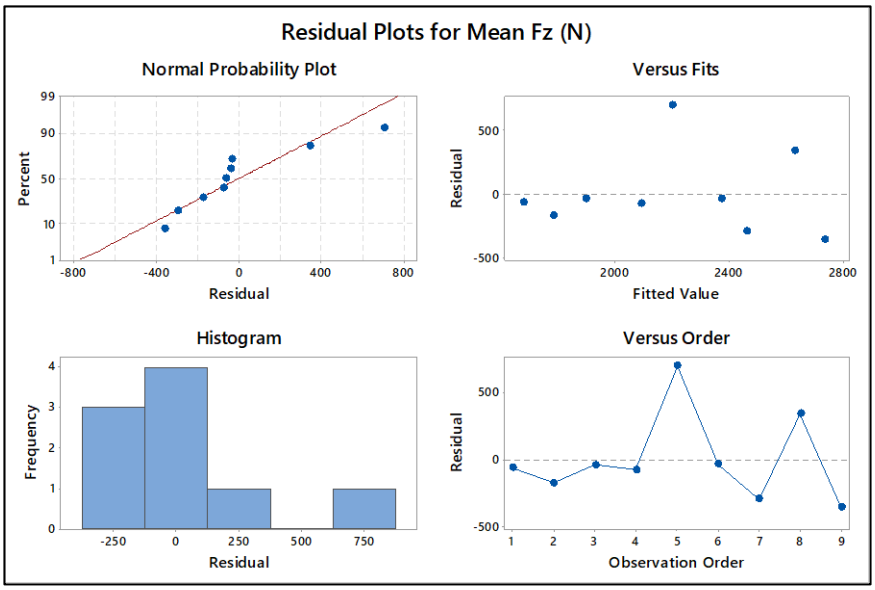

Figure 4.20. Residual plots for Force-mean of The Second Group.

4.6.6. Moment-Mean Analysis of First Group Using Taguchi Method

Figure 4.21 (a) and (b) show the optimal values of feed rate, cutting speed, and steps with Moment-Mean analysis of the first group using the Taguchi method, it was 0.2 mm/min, 768 rpm, and 10 mm respectively. Residual plot for Moment-Mean of the first group in Figure 4.22. The typical Probability Plot displays the individual value

departure from the regression model equation. The low deviation is visible at closely spaced places surrounding the line.

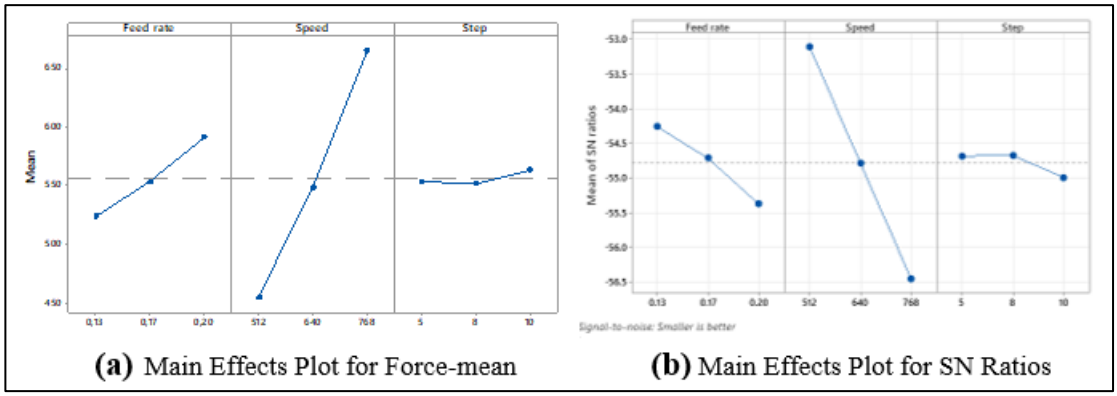

Figure 4.21. Main Effects Plot for Moment-Mean and SN Ratios of The First Group

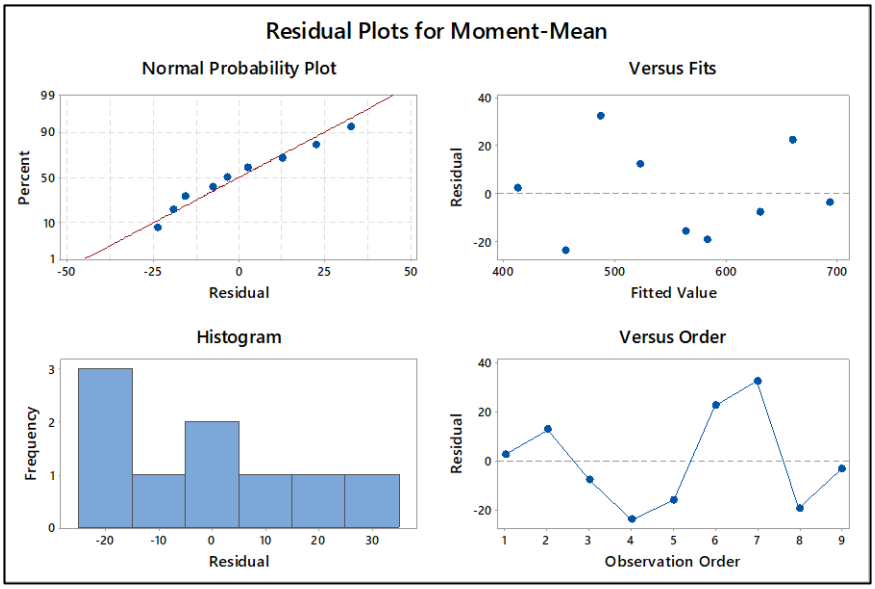

Figure 4.22. Residual plots for Moment-Mean of The First Group.

4.6.7. Moment-Mean Analysis of Second Group Using Taguchi Method.

Figure 4.23 (a) and (b) derived by Taguchi analysis, illustrates the relationship between the Moment-Mean findings of the second group and the three parameters of feed rate, cutting speed, and step for the first group experiments. The cutting speed, feed rate, and step parameters all had maximum values of 0.3 mm/min, 1766 rpm, and 10 mm, respectively. It has been adequately demonstrated that these values are the perfect

ones. Figure 4.24 shows the Residual plot for the Moment-Mean of the Second group, it was a small difference as some results diverged obtained from those of the first group. on the other hand, In the rest of the experiments, in comparison to the equation of the regression model, the normal probability plot displays the individual value's deviation. Low deviation can be seen at closely spaced places around the line.

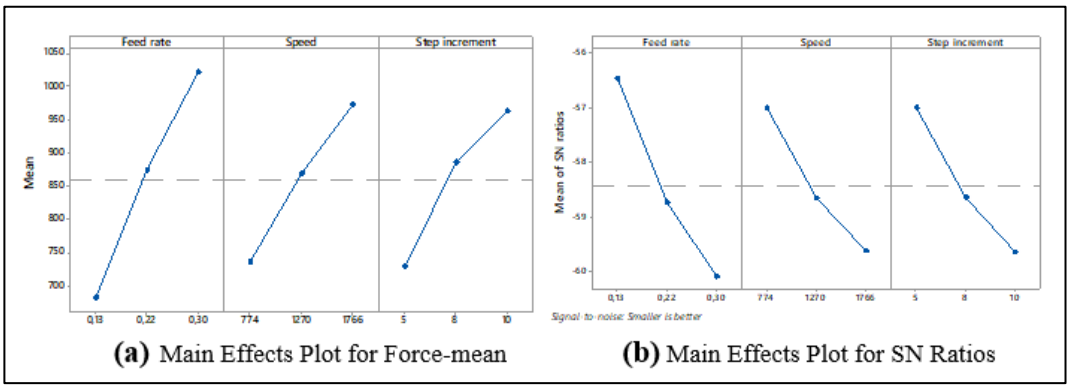

Figure 4.23. Main Effects Plot for Moment-Mean and SN Ratios of Second Group

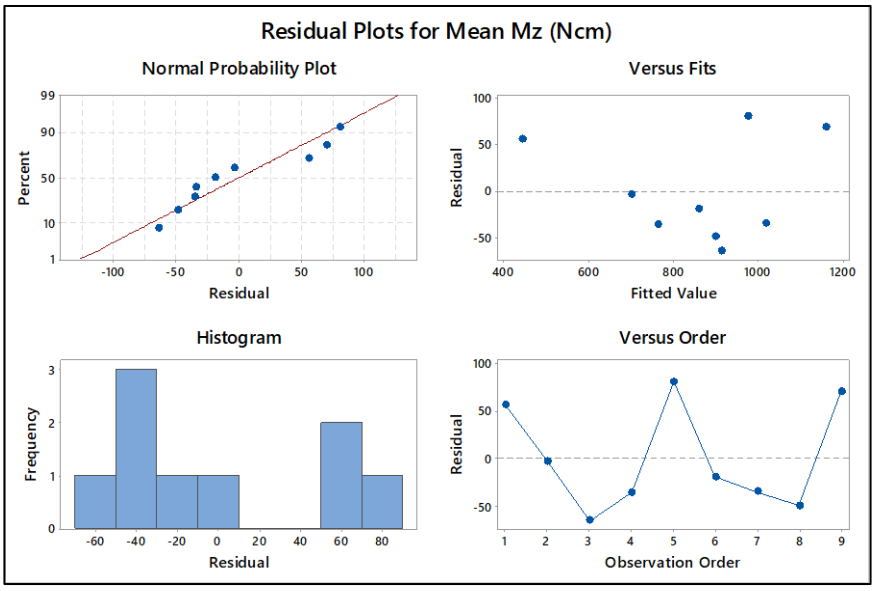

Figure 4.24. Residual plots for Moment-Mean of The Second Group.

4.6.8. Comparison Between Force-mean and Moment-Mean Taguchi Analysis of First and Second Group

According to the results obtained from Force-mean and Moment-Mean using Taguchi analysis of First and Second Group experiments the following can be summarized:

- ✓ The idealism feed rate of the first group according to Force-mean and Moment-Mean was 0.2 mm/min while 0.3 mm/min of the second group.
- ✓ Cutting speed idealism to Force-mean was 670 rpm for the First Group and 1270 rpm for the Second Group.
- ✓ Cutting speed idealism to Moment-Mean was 768 rpm for the First Group and 1766 rpm for the Second Group.
- ✓ The idealism steep according to Force-mean and Moment-Mean was 10 mm for both groups in all analysis

4.7. 3D SURFACE ILLUSTRATION

By examining a three-dimensional surface of the anticipated response, the 3D Surface Plot function in the Minitab software allows you to investigate a response variable's (Z) link to two predictor variables (X and Y). There is an option of representing the anticipated reaction as a wireframe or a smooth surface.

4.7.1. 3D Surface Plotter of Ra for First Group

First, the findings produced in accordance with Figure 4.25 demonstrate the correlation between the Ra results and two of the first group's cutting parameters (the Feed Rate and step). based on the forecasts obtained as displayed in Figure 4.25 (a). The lowest expected value of Ra is seen at a step size of 10 mm with a feed rate of 0.2 mm/min, but it grew with a decrease in feed rate to reach about 2.5 μm at steps of 5 and 10 mm. While the feed rate ranged from 1.6 to 1.8 mm/min for all steps, the prediction of Ra's results was practically convergent at 1.5 mm.

Second, it is obvious from the data in Figure 4.25 (b), that the greatest Ra average result is about 2.5 μm at 500 rpm with a feed rate of 0.12 mm/min, while the lowest value was almost 1.4 μm at the same cutting speed with a feed rate of 0.2 mm/min. The relationship between Ra average results predictions and cutting speed and step may be seen in Figure 4.25 (c).

This clearly demonstrates the inverse relationship between Ra value predictions, cutting speed and steepness. Specifically, the higher cutting speed rate and the lower the step value, the higher Ra result; conversely, the lower the cutting speed rate and the higher step value, the lower Ra result. Its highest prospect was measured at 500 rpm with 5 mm and 800 rpm with 10 mm, and its lowest prospect was measured at 500 rpm and 10 mm, cutting speed and steep, respectively, at 0.4 μm.

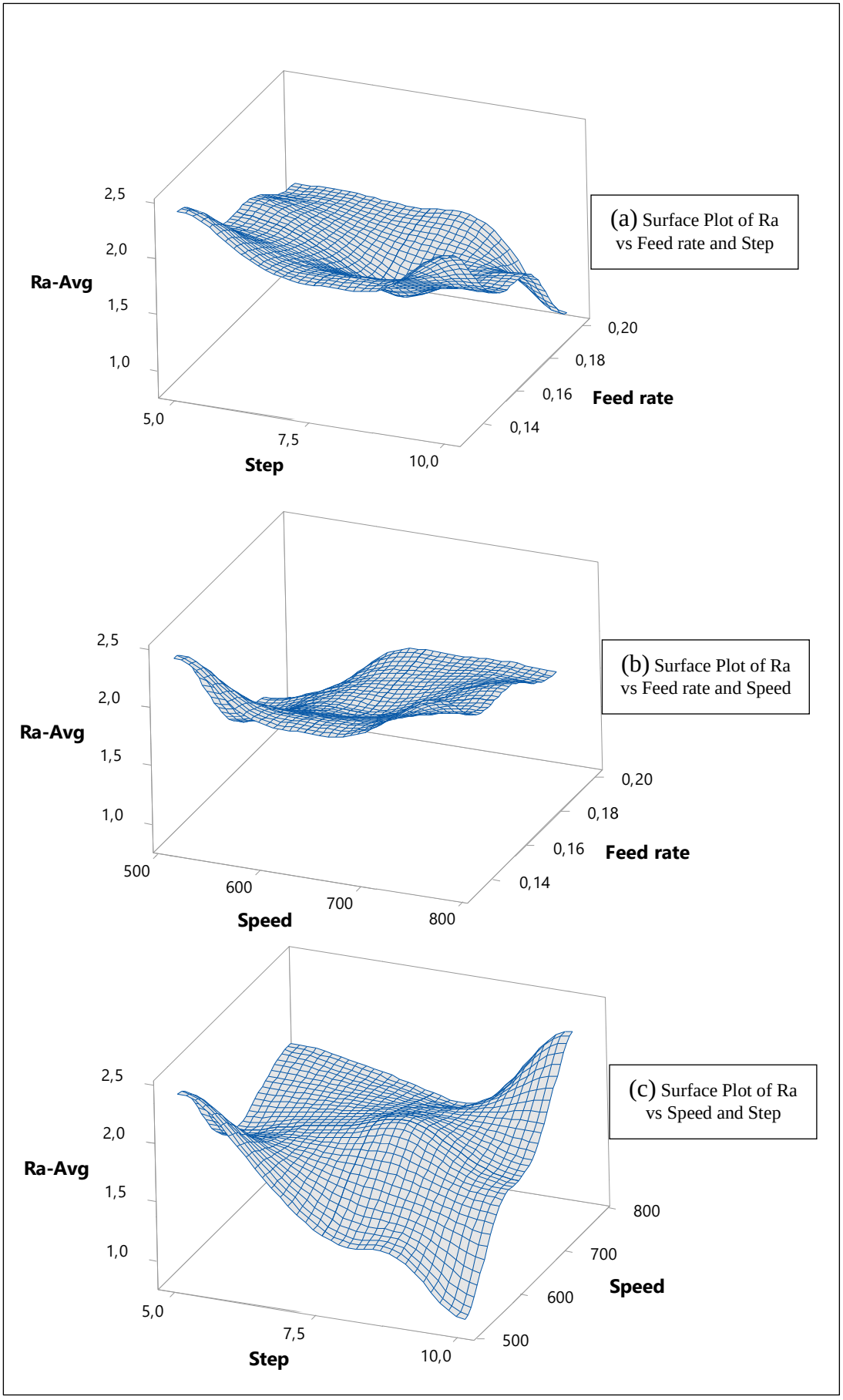

Figure 4.25. 3D Surface Plotter of Ra for First Group.

4.7.2. 3D Surface Plotter of Ra for Second Group

First, the findings produced in accordance with Figure 4.26 demonstrate the correlation between the Ra results and (the Feed rate and cutting speed) of the Second group. Based on the reached predictions, as seen in Figure 4.26 (a), the lowest expected value of Ra is observed at cutting speed of 800 rpm and at feed rate of 0.1 mm/min. While increased as the feed rate and cutting speed were increased reaching almost 2.2 μm at the cutting speed of 1200 rpm and 0.1 mm/min as well as 2.2 μm at 800 rpm with feed rates 0.25 and 0.3 mm/min.

From Figure 4.26 (b) it is obvious that the greatest Ra average result is about 2.4 at steep 7 mm with a feed rate of 0.1 mm/min, while the lowest value was almost 1.2 μm at a feed rate of 0.3 mm/min with a steep of 10 mm.

The relationship between Ra average results predictions, cutting speed and step were shown in Figure 4.26 (c). In particular, the Ra result was 2.2 μm at 1800 rpm with a step of 10 mm, and the higher the cutting speed value, the higher the result. The lowest value was at 500 rpm, which was over 1.2 μm. However, the highest prospect was measured at 1200 rpm, with a 7 mm steep.

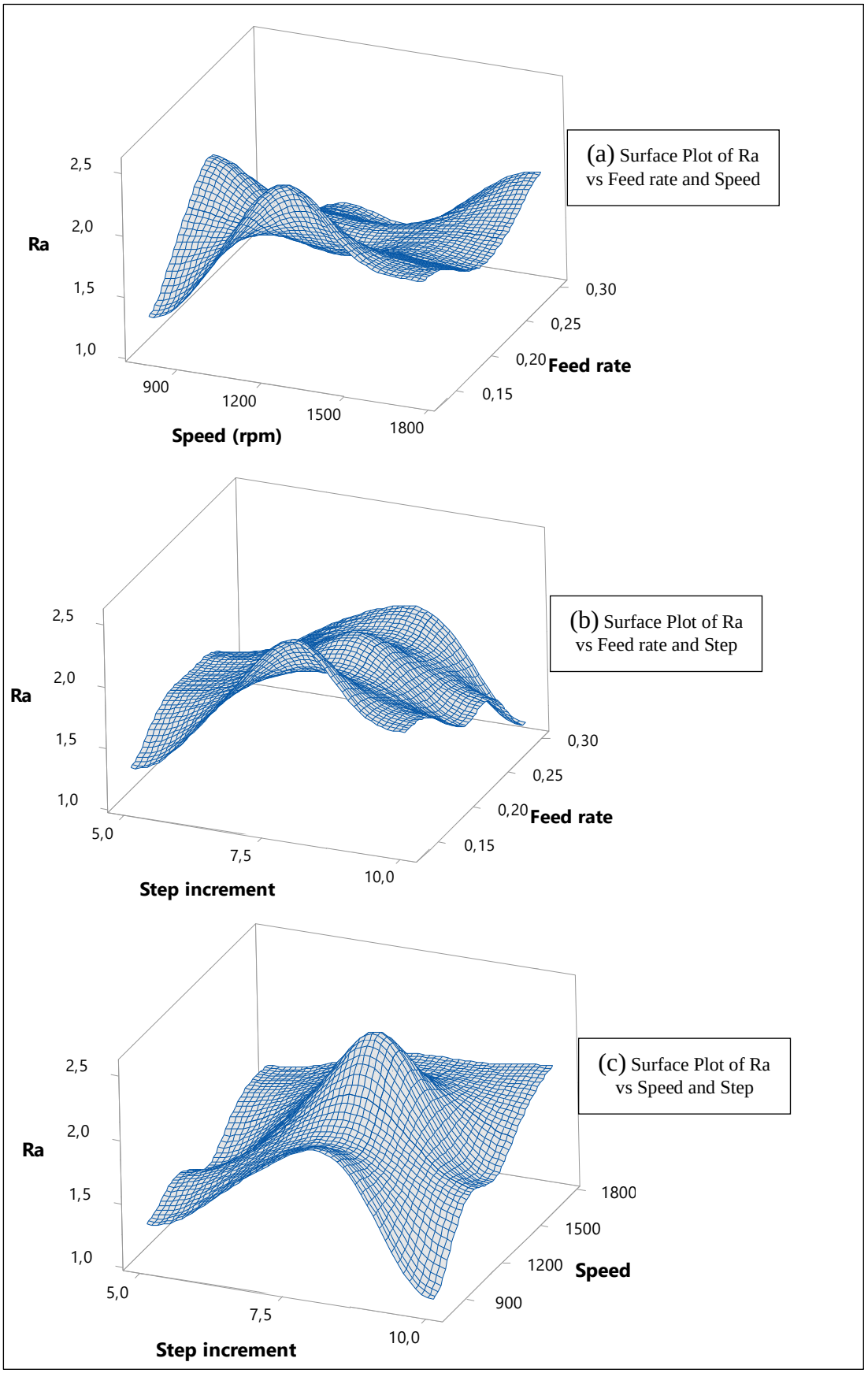

Figure 4.26. 3D Surface Plotter of Ra for Second Group.

4.7.3. Comparison Between 3D Surface Plotter of Ra for First and Second Group

According to the results of the 3D surface plotter, the relationship between Ra and cutting parameters of first and second groups' experiments were summarized in the following points.

- ✓ The highest expected value of Ra of the first group was almost nearly 2.5 μm, while the lowest expected value was about 0.5 μm. The Ra prophecies ranged between 1 to 1.6 μm.
- ✓ The highest expected value of Ra of the second group was nearly 2.3 μm, while was the lowest expected value 0.7 μm. The Ra prophecies were ranged between 1.2 to 2 μm.

4.7.4. 3D Surface Plotter of Force-mean for First Group

When the feed rate and cutting speed are reduced, the force Force-mean predictions become less, as can be seen from the prospective results acquired regarding the relationship between these two cutting parameters for the first group, as shown in Figure 4.27 (a). For instance, the lowest predicted value of Force-mean was around 1000 N when the feed rate and speed were 0.1 mm/min and 500 rpm, respectively.

The higher results were at 0.2 mm/min with 7.5 mm in Figure 4.27 (b) and 0.15 mm/min with 5 mm around 2200 N. The following predictions were made regarding the interaction between the force Force-mean and (the Feed Rate and steep). However, the projected value for the Force-mean was at 0.1 mm/min and 5 mm, or 1000 N.

The relationship between the Force-mean and the cutting speed and the step are shown in Figure 4.27 (c). At 500 rpm with a 5 mm Force-mean, the cutting force is around 50 N, while at 600 rpm with a 7.5 mm, it was around 1500 N. The factors that predicted the least cutting force were lower cutting speed and decreasing steep values. Additionally, at an 800-rpm cutting speed with steep 5 and 7.5 mm, the highest Force-mean values projected were around 2200 N.

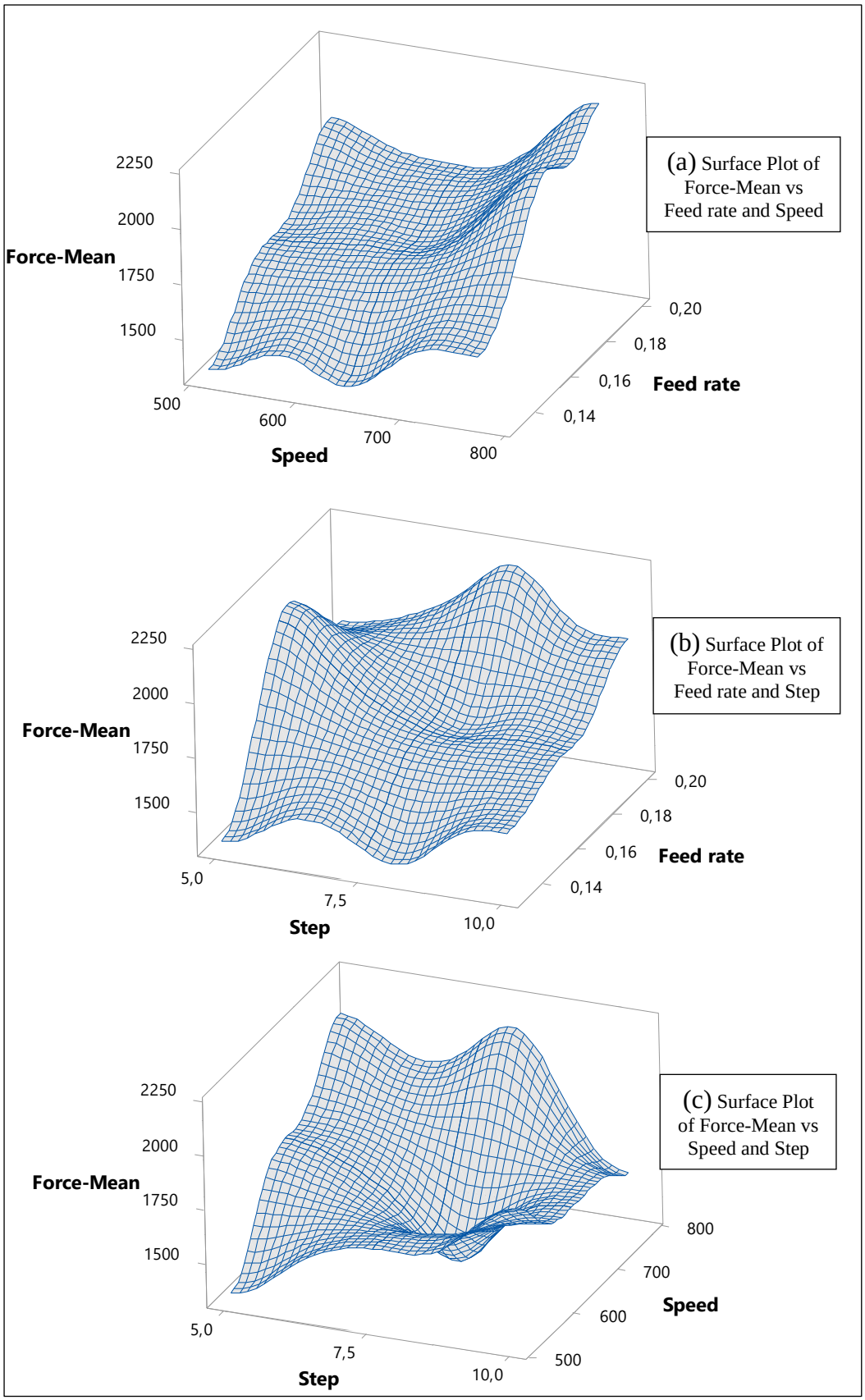

Figure 4.27. 3D Surface Plotter of Force-mean for First Group.

4.7.5. 3D Surface Plotter of Force-mean for Second Group

Figure 4.28 (a) shows the relationship between the force Force-mean, the cutting speed, and the cutting steep. The highest value was at 0.3 mm/min with 1200 rpm and around 2900 N. On the other side, the lowest value was 1600 N at 0.1 mm/min with 800 rpm. generally, an increase in the feed rate and cutting speed Leads to Increase values Ra results.

Expectations of the Feed Rate, Steep, and Force-mean relationship with a rising in feed rate and a fall in steepness. A very high result was obtained, with the peak reaching roughly 3000 N at a feed rate of 0.3 mm/min and steepness of 5 mm. However, as seen in Figure 4.28 (b), the majority of the expectations were between 2000 and 2500 N.

Figure 4.28 (b) illustrates how expectations of the relationship between cutting speed, steep, and Force-mean visibly fluctuated. For instance, Force-mean projected at a cutting speed of 1200 rpm with a steep of 5 and 10 mm was 3000 N, while at the same speed but with a steep of 7.5 was about 1500 N.

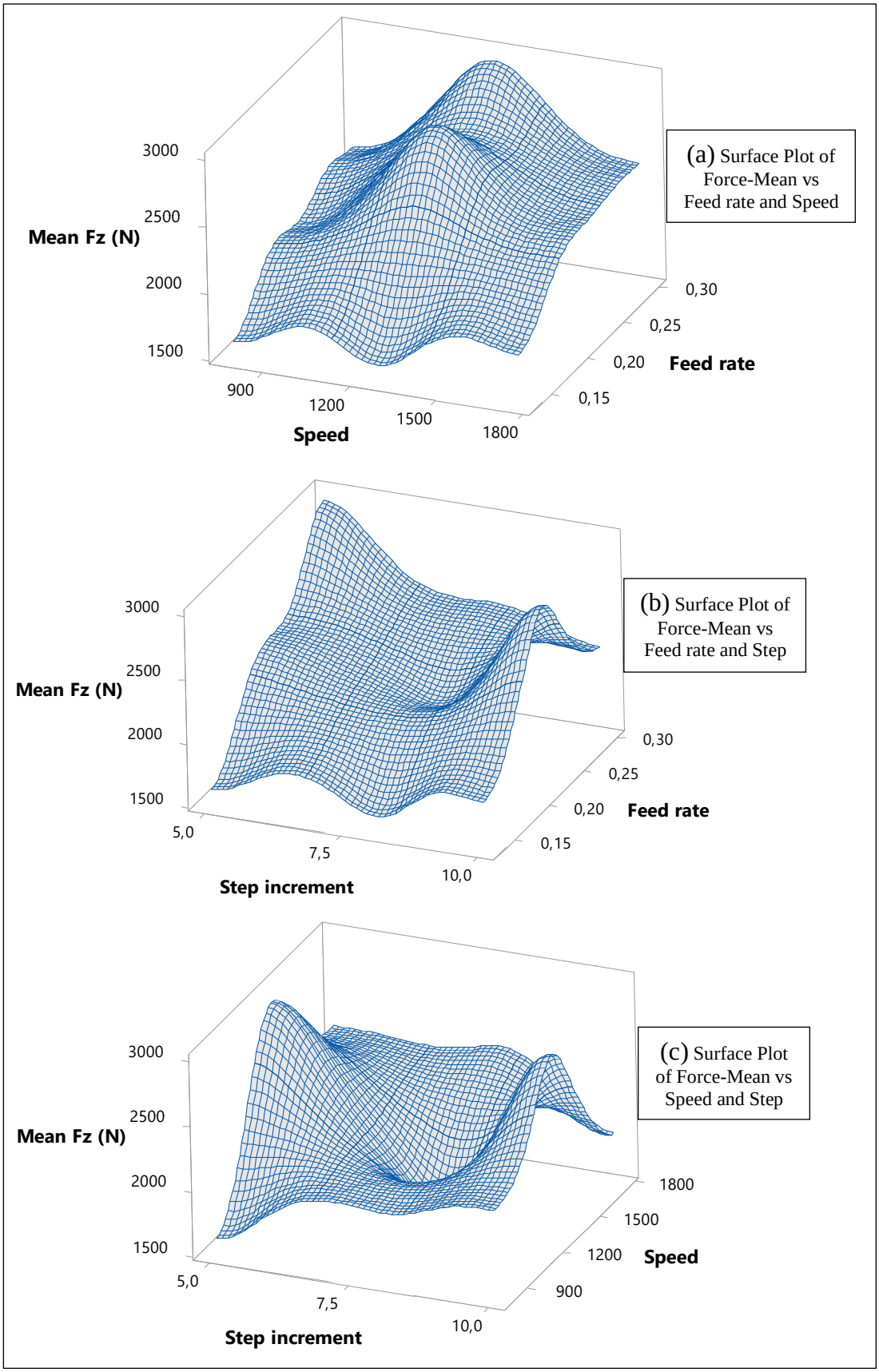

Figure 4.28. 3D Surface Plotter of Force-mean for Second Group.

4.7.6. 3D Surface Plotter of Moment-Mean for First Group

The relationship between the Moment-mean and two cutting parameters for the first group of feed rate and cutting speed is presented in Figure 4.29 Regarding Figure 4.23 (a), the lowest expected value of Moment-mean was 400 Ncm at 0.12 mm/min with 500 rpm of the feed rate and cutting speed, and the highest value was at 0.2 mm/min with 800 rpm of the feed rate and cutting speed, respectively. Furthermore, the Moment-mean expected value at 0.1 mm/min with 800 rpm and 0.2 mm/min with 500 rpm was virtually identical to 680 Ncm. The association between the Moment-mean and two additional cutting parameters is seen in Figure 4.29 (b). Although, the Moment-mean disturbance was more pronounced at 0.16 and 0.2 mm/min with 5 and 7.5 mm, there was a noticeable increase for some cutting parameters a little over 690 Ncm. However, the projection value was 500 Ncm at 0.16 mm/min and 7.5 mm.

For the majority of cutting parameter values, the association between the Moment-mean and the two cutting parameters (the cutting speed and the steep) was reliable. The values of Moment-mean were expected to rise with higher cutting speeds and decrease with lower cutting speeds. The projected high value was at 800 rpm, but the majority of the step values for Moment-mean were about 650 Ncm, Moment-mean was between 400 and 500 at 500 rpm for the bulk of step values as shown in Figure 4.29 (c).

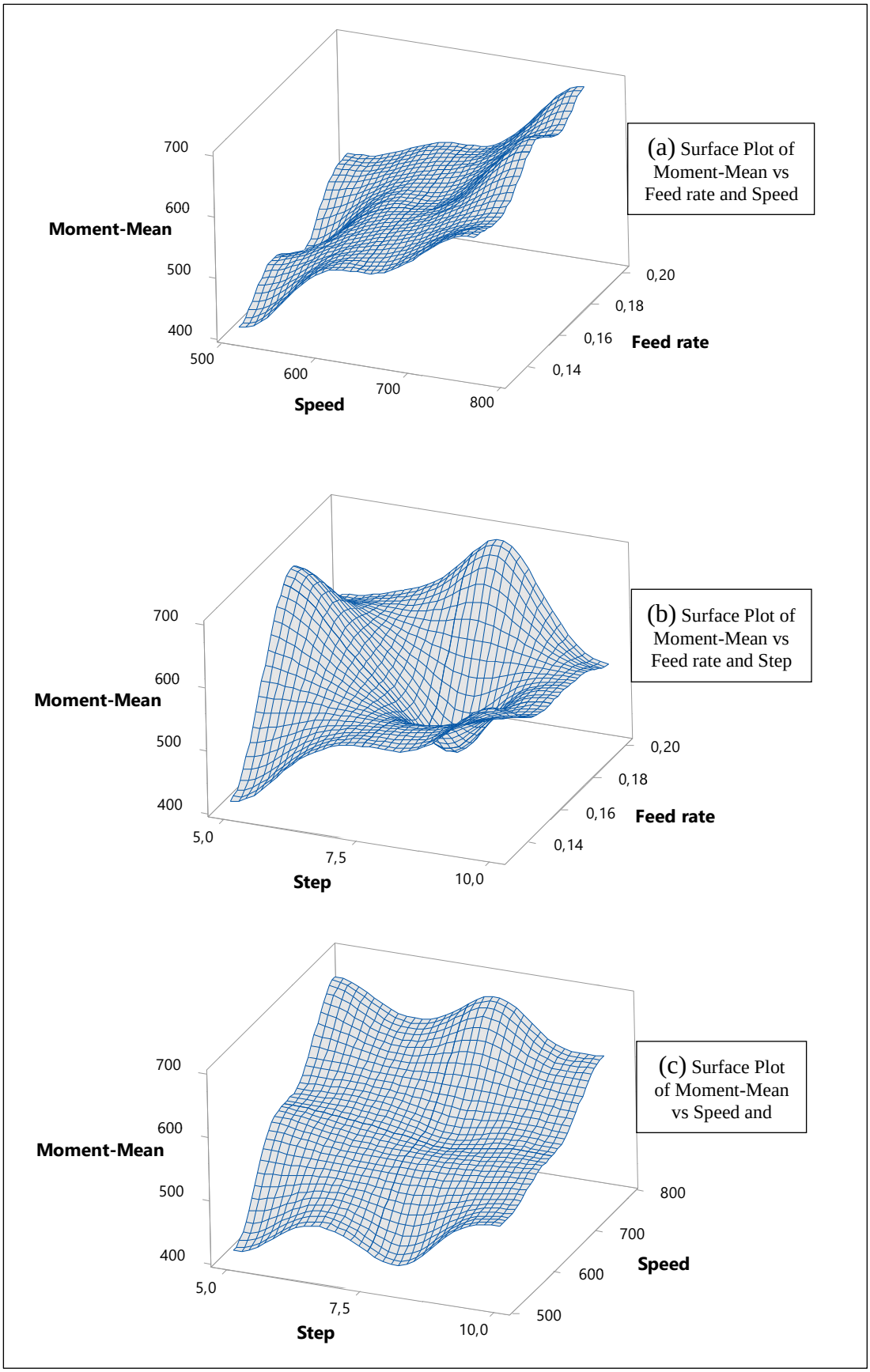

Figure 4.29. 3D Surface Plotter of Mz for First Group.

4.7.7. 3D Surface Plotter of Moment-Mean for Second Group

Generally, in Figure 4.30 (a) the feed rate and cutting speed are reduced and the force Moment-Mean prediction becomes less. This is clearly appeared from the prospective results acquired regarding the relationship between the feed rate, cutting speed, and Moment-Mean. Moment-Mean projected at a feed rate of 0.1 mm/min with a cutting speed of 800 rpm is 500 Ncm which record the lowest value. On other hand, the Moment-Mean projected at a feed rate of 0.3 mm/min with a cutting speed of 1800 rpm is 1250 Ncm.

Figure 4.30 (b) showed the relationship between the Moment-mean, the feed rate, and steep. The lowest value was around 500 Ncm at the feed rate of 0.1 mm/min with steep 5 mm and the higher value 1250 Ncm was at 0.3 mm/min with 7.5 mm.

The relationship between the Moment-mean, the cutting speed, and the step was depicted in Figure 4.30 (c), which was extremely similar to Figure 4.30 (b). The lowest value was around 500 Ncm at a cutting speed of 800 rpm with a 5 mm pitch, and the highest value was 1250 Ncm at a cutting speed of 1800 rpm with a 7.5 mm pitch. The remaining expectations ranged from 750 to 100 Ncm.

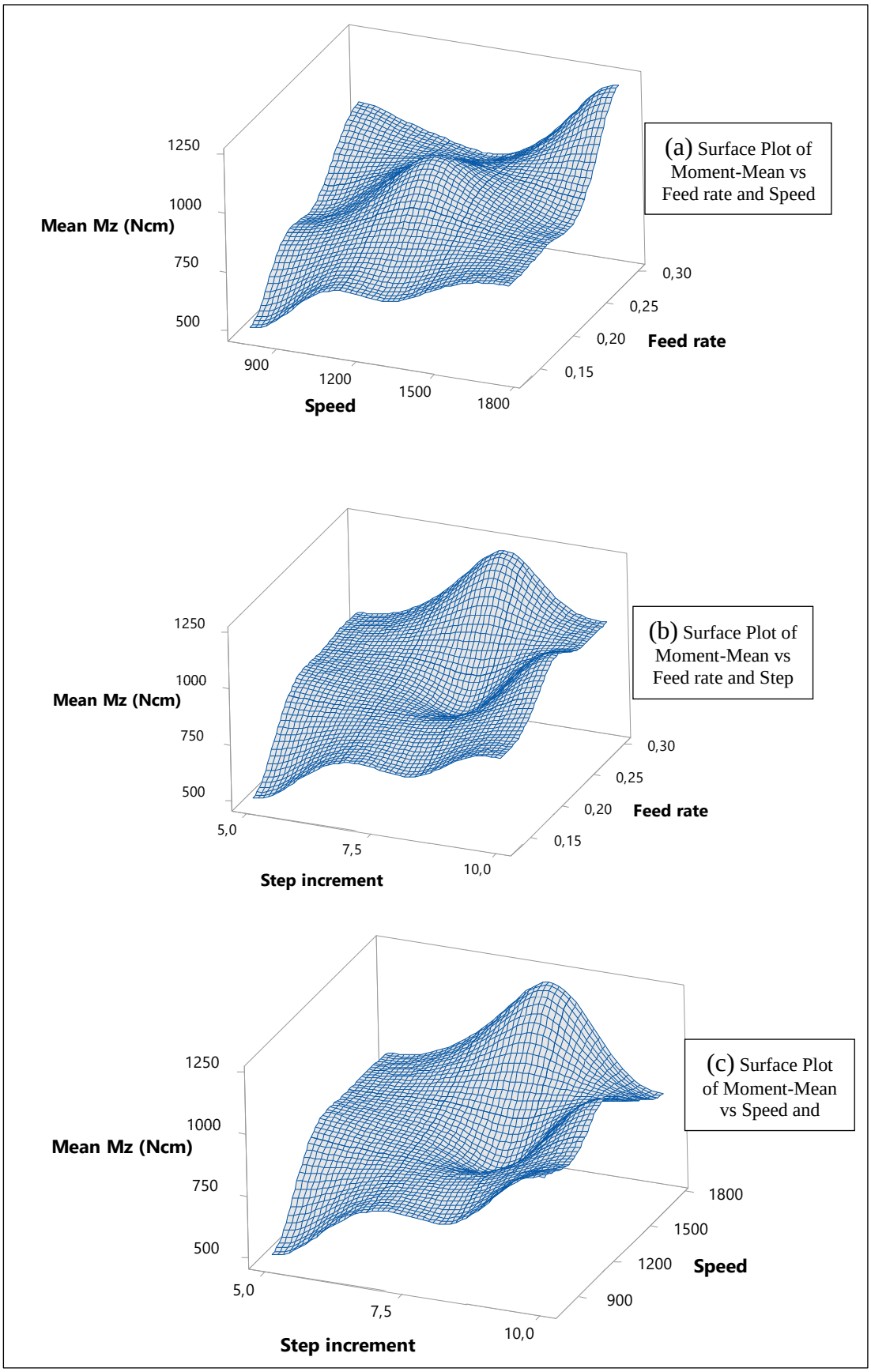

Figure 4.30. 3D Surface Plotter of Mz for Second Group.

4.7.8. Comparison Between 3D Surface Plotter of Fz and Mz for First and Second Group

According to the results of the 3D surface plotter of the relationship between Force-mean and Moment-mean with cutting parameters of the first and second groups' experiments were summarized in the following points.

- ✓ The highest expected value of Force-mean of the first group was 2250 N, while the lowest value about 500 N. Most of Fz prophecies were ranged between 1600 to 1800 N.
- ✓ The highest value of Force-mean of the second group was 3000 N, while the lowest value was about 1500 N. Most of Fz prophecies were ranged between 1900 to 2100 N.
- ✓ The highest value of Moment-mean of the first group was about 400 Ncm, while the lowest value about 400 Ncm. The values of Fz prophecies were ranged between 450 to 550 Ncm.
- ✓ The highest value of Moment-mean of the second group was about 1200 Ncm, while the lowest value was about 500 Ncm. The values of Fz prophecies were ranged between 600 to 800 Ncm.

PART 5

CONCLUSION AND RECOMMENDATIONS

5.1. CONCLUSION

The methodology for investigating the impact of parameter levels on experimental findings in drilling procedures is presented in this study. The optimization is based on the experimental work applied on AISI 403 stainless steel in order to raise the standard of drilling products. Firstly, design two different experimental drillings using the Taguchi method, the first group consists of close parameter levels that increase and decrease by 20% to the parameters following the computation of speed and feed, while the second group consists of distant parameter levels that increase and decrease by 40% to the parameters. Secondly, the experimental drilling was done by a numerical control milling machine (CNC). After that, the Minitab software used the Taguchi method for experimental design. Finally, analysis of variance (ANOVA) and Taguchi analysis to compare experimental results.

The results analysis found significant differences between the experimental results for surface roughness (Ra), force-mean (Fz), and moment-mean (Mz), which were recorded and analyzed in this study. In experiment number 7, "Ra" values declined in both groups when the cutting speed was 512 rpm with a feed rate of 0.2 mm/min. In the first group, however, the cutting speed was 774 rpm with a feed rate of 0.3 mm/min., this resulted in satisfactory "Ra" values. However, when employing the cutting speeds of 640 and 1270 rpm with feed rates of 0.17 and 0.22, implausible results were produced in experiment number 5, where both groups showed virtually

the same "Ra" values. While experiments 2 and 1 in the first and second groups, respectively, generated the highest value for Ra findings.

According to the results obtained from Ra Taguchi's analysis of the first and second groups, it was noted that the best results were with the highest feeding rate and the lowest speed for the two groups. The best outcome, however, was for the first group with the highest step, as opposed to the second group with the lowest step. But, according to the results of the 3D surface plotter the relationship between Ra and cutting parameters of the first and second groups' experiments was the highest expected value of Ra of the first group was almost nearly 2.5 μm, while the lowest expected value was about 0.5 μm. The Ra prophecies ranged between 1 to 1.6 μm. The highest expected value of Ra of the second group was nearly 2.3 μm, while was the lowest expected value 0.7 μm. The Ra prophecies ranged between 1.2 to 2 μm.

The first and second groups' experimental results show that the force (Fz and Mz) rises as the feed rate rises because the cutting tool is trying to remove more material. With higher feed rates comes a higher material removal rate (MRR). The first three studies also showed that the lowest values for both groups were quite close to one another. For instance, in the first experiment, the first and second groups' Mz 413.9 and 487.5 MN closely paralleled Fz 1612 and 1346 N. However, Similar outcomes were found when looking at all of the first group's experiments, with Fz varying from 1000 to 2200 N and Mz varying from 400 to 700 Ncm. The second group did, however, increase its Mz and Fm force after the sixth experiment, peaking at almost 3000 N for Mz and 1250 Ncm for Fz. In both groups, the feeding rate was 0.13 mm/min, so the outcome was remarkably similar to experiment number 1. This suggests that the force as a whole was significantly impacted by the feeding rate.

According to the results obtained from Force-mean and Moment-Mean using Taguchi analysis of First and Second Group experiments, the idealism feed rate of the first group according to Force-mean and Moment-Mean was 0.2 mm/min while 0.3 mm/min of the second group. Cutting speed idealism to Force-mean was 670 rpm for the First Group and 1270 rpm for the Second Group. Cutting speed idealism to Moment-Mean was 768 rpm for the First Group and 1766 rpm for the Second Group.

The idealism steep according to Force-mean and Moment-Mean was 10 mm for both groups in all analyses.

The first and second groups' ANOVA findings. The first group's cutting speed had the greatest percentage impact on the Ra results (64.48%), while the second group had the greatest percentage impact on the cutting parameters (60.92%). Ra is least affected by the cutting speed rates of 14.54 and 10.91% in the first and second groups. As for Force-mean and Moment-mean, the feed rate had the greatest influence on Force-mean between 65% and 60% in both the first and second groups' tests. However, the moment mean was used for the cutting speed and feed rate, which were 47% and 87.4%, respectively. However, with an effective ratio that varied only between 0.1% and 23%, the steep impact on Force-mean and Moment-mean in both groups was the least significant of all the cutting factors. But, The results of the 3D surface plotter of the relationship between Force-mean and Moment-mean with cutting parameters of the first and second group’s experiments were summarized in the following points. The highest expected value of Force-mean of the first group was 2250 N, while the lowest value was about 500 N. Most of Fz prophecies ranged between 1600 to 1800 N. The highest value of Force-mean of the second group was 3000 N, while the lowest value was about 1500 N. Most of Fz prophecies were ranged between 1900 to 2100 N. The highest value of Moment-mean of the first group was about 400 Ncm, while the lowest value was about 400 Ncm. The values of Fz prophecies ranged between 450 to 550 Ncm. The highest value of Moment-mean of the second group was about 1200 Ncm, while the lowest value was about 500 Ncm. The values of Fz prophecies ranged between 600 to 800 Ncm.

With 512 rpm cutting speed and various feed rates, tests 1, 4, and 7 yielded the best chips from the first experimental group. While experiments 1 and 5 generated the best chips from the second experiment group with cutting speeds of 774 and 1270 rpm and feed rates of 0.13 and 0.22 mm/min, respectively.

5.2. RECOMMENDATIONS

The recommendations are summarized in the following points:

- ✓ Using hardness minerals for the future studies
- ✓ focuses on Study tool wear and live tool (drill) In future studies.
- ✓ Comparison between surface roughness and machine time.

REFERENCES

1. Emin Salur, Abdullah Aslan, Mustafa Kuntoglu, Aydın Gunes, Omer Sinan Sahin, "Experimental study and analysis of machinability characteristics of metal matrix composites during drilling", **http://people.hofstra.edu/geotrans/eng/ methods / ch1m2en.html** 166 (2019) 401- 413.

2. A. Z. Sultana, Safian Sharifb, Denni Kurniawanb., "Chip Formation When Drilling AISI 316L Stainless Steel using Carbide Twist Drill", ***2nd International Materials, Industrial, and Manufacturing Engineering Conference MIMEC 2015,*** 4-6 February 2015, Bali Indonesia.

3. M. SenthilKumar, A.Prabukarthi, V.Krishnaraj, "Study on Tool Wear and Chip Formation during Drilling Carbon Fiber Reinforced Polymer (CFRP)/ Titanium Alloy (Ti6Al4V) Stacks", ***International Conference On DESIGN AND MANUFACTURING,*** 64 (2013) 582 – 592.

4. U. Çaydaş, Ahmet Hasçalık, Ömer Buytoz, and Ahmet Meyveci,"Performance Evaluation of Different Twist Drills in Dry Drilling of AISI 304 Austenitic Stainless Steel", ***Materials and Manufacturing Processes,*** 26: 951–960, 2011.

5. Eyup Bagci, Babur Ozcelik, "Analysis of temperature changes on the twist drill under different drilling conditions based on Taguchi method during dry drilling of Al 7075-T651", **Int J Adv Manuf Technol** (6 July 2005).

6. Ajay Kumar Singh, Nishant Moona ,, "Design of a Universal Micro Radial Drilling Machine", Lecturer Notes, ***IJSTE - International Journal of Science Technology & Engineering***, Boston, Issue 09 (March 2016).

7. S.O. Banjo1, O.O. Joseph1, O.S.I. Fayomi1, M. Udor1, J.O. Dirisu1, D.O. Omole2, S.A. Afolalu1, I. Osagie3., "Evaluation of a constructed manual drilling machine for small scale operation", **International Conference on Engineering for Sustainable World** (ICESW 2020).

8. R.D. Mardane1 Prof. U.D. Gulhane2 Dr.A.R. Sahu3., "Conceptual Design of Automated Attachment for Positioning Bed of Drilling Machine with Respect to Cad Model", **IJSRD - International Journal for Scientific Research & Development** (Issue 10, 2015).

9. Internet: **https://learnmechanical.com/drilling-machine/** (2022).

10. Internet: ***https://shikshartin.wordpress.com/1-4/mtt/drill/sensitive-drill machine*** (2022).

11. Mostafa Piri a, Reza Mikaeil b, Hamid Hashemolhosseini c, Alireza Baghbanan d, Mohammad Ataei e., "Study of the effect of drill bits hardness, drilling machine

operating parameters and rock mechanical parameters on noise level in hard rock drilling process", ***Measurement*** (2021).

12. Internet: ***//https://www.indiamart.com/proddetail/38mm-pillar-type-drilling machine-6365688388.html*** (2022).

13. U. Hema Nikhitha, "Design of 360 Degree Flexible Drilling Machine" International ***Journal of Engineering Research & Technology (IJERT)***, 8 Issue (01, January-2019).

14. Internet: //***https//www.knuth.com/en/machines/drilling/radial-drillingmachines*** (2022).

15. Internet: ***//https://www.indiamart.com/ckp-industries/gang-drillingmachines. html (***2022).

16. Internet: ***//https: // www.kingsang.com.tw/eg/product_a2.html*** (2022).

17. YogendraTyagi1, Vedansh Chaturvedi2, Jyoti Vimal3., "Parametric optimization of CNC Drilling machine for mild steel using Taguchi design and Single to Noise ratio Analysis", ***International Journal of Engineering Science and Technology (IJEST)*** (August 2012).

18. Internet: ***//https:// www.openpr.com/news/1835860/computer-numerical-control -machines-market-key-players*** (2020).

19. Yogendra Tyagi, Vedansh Chaturvedi2 and Jyoti Vimal3., "A Review on Multi Spindle Drilling Special Purpose Machine with Respect to Productivity", ***IJSRD - International Journal for Scientific Research & Development*** Issue 08 (2015).

20. Internet: ***//https://www.exportersindia.com/indian-suppliers/spm-drill-machine .htm*** (2022).

21. Dhanraj Patel1 and Rajesh Verma2., "Analysis of Drilling Tool Life A Review", ***International Journal of Mechanical Engineering and Robotics Research*** Issue ISSN 2278 – 0149 (2015).

22. A. Z. Sultana, Safian Sharifb and Denni Kurniawanb., "Chip Formation When Drilling AISI 316L Stainless Steel using Carbide Twist Drill", ***Procedia Manufacturing***, (2015).

23. Internet: ***https :// chainheadway.com/latest-news/tungsten-carbide-drill/*** (2022)

24. E. Abele and M. Fujara., "Simulation-based twist drill design and geometry optimization", ***CIRP Annals - Manufacturing Technology***, (2010).

25. Internet: ***https://cuttingtools.ceratizit.com/tr/en/machining-know-how /drilling /advisor/drill-geometry.html*** (2022).

26. Minitab. Wiley Interdisciplinary Reviews: Computational Statistics., “Simulation -based twist drill design and geometry optimization”, ***Minitab Aylin Alin*****,** (November/December 2010).

27. Internet: ***https: // www.minitab.com/en-us/products/minitab/*** (2022).

28. Internet: ***https: //matmatch.com/learn/material/aisi-304-stainless-steel*** (2022).

29. B.M. Gonzalez a, C.S.B. Castro a, V.T.L. Buono a, J.M.C. Vilela b, M.S. Andrade b, J.M.D. Moraes c, M.J. Mantel d., “The influence of copper addition on the formability of AISI 304 stainless steel”, ***Materials Science and Engineering*****,** A343 (2003).

30. Internet: ***https://matmatch.com/learn/material/aisi-304-stainless-steel*** (2022).

31. M. El Wahabi a, J.M. Cabrera a, b, J.M. Prado a, b., “Hot working of two AISI 304 steels: a comparative study”, ***Materials Science and Engineering*** Issue A343 (2003).

32. Atul Kulkarnia,Vikas Sargadeb ,and Chittaranjan Morea., “Machinability Investigation of AISI 304 Austenitic Stainless Steels using Multilayer AlTiN/TiAlN Coated Carbide Inserts”, ***Procedia Manufacturing*** (2018).

33. Internet: ***https://www.azom.com/article.aspx?ArticleID=965*** (2022).

34. Internet:***https://www.jayeshmetal.com/stainless-steel-304-304l-fasteners manufacturer-supplier.html*** (2022).

35. Internet: ***https://varadprocess.com/heat-exchanger-manufacturers-pune/(2022***).

36. Internet: ***https://www.rsametal.com.tr/en/stainless-steel-304.php*** (2022).

37. Mustafa Kurt, Eyup Bagci and Yusuf Kaynak ., “Application of Taguchi methods in the optimization of cutting parameters for surface finish and hole diameter accuracy in dry drilling processes”, ***Int J Adv Manuf Technol*** (2008).

38. E. Kilickap,“Optimization of cutting parameters on delamination based on Taguchi method during drilling of GFRP composite”, ***Expert Systems with Applications*** (2010).

39. Adem Çiçek, Turgay Kıvak, Gürcan Samtaş, “Application of Taguchi Method for Surface Roughness and Roundness Error in Drilling of AISI 316 Stainless Steel”, ***Strojniški vestnik - Journal of Mechanical Engineering*** Issue 58(2012).

40. B. Ramesh and A. Elayaperumal.,“Optimization Of Process Parameter Levels During Drilling High Fiber Volume Fraction Nonlaminated GFRP Polymeric Composites ”, ***International Journal of Science and Engineering Applications (IJSEA)*** (2012).

41. K. Lipin and Dr. P. Govindan, " A Review on Multi Objective Optimization of Drilling Parameters Using Taguchi Methods", ***A K G E C Jour of Technology*** (2013).

42. H Prakash1., "Investigation to Study the Effect of Drilling Process Parameters on Surface Finish Using Taguchi Method", ***International Journal of Mechanical Engineering and Robotics Research*** (2014).

43. Palanisamy Shanmughasundarama and Ramanathan Subramanian., "Study of parametric optimization of burr formation in step drilling of eutectic Al–Si alloy–Gr composites", ***jmr&t Journal of Materials Research and Technology*** (2014).

44. J.Udaya Prakash and Perumal Sudalai., " Optimization of Machining Parameters in Drilling***", International Journal of Applied Engineering Research of Aluminium Matrix Composites using Taguchi Technique*** ISSN 0973-4562 (2015).

45. A.T. Kuzu, K. Rahimzadeh Berenji, B.C. Ekim, M. Bakkal., "The thermal modeling of deep-hole drilling process under MQL condition", ***Journal of Manufacturing Processes*** 29 (2017).

46. Güven Meral, Murat Sarıkaya, Mozammel Mia, Hakan Dilipak, Ulvi Şeker, Munish K. Gupta., "Multi-objective optimization of surface roughness, thrust force, and torque produced by novel drill geometries using Taguchi-based GRAI", ***The International Journal of Advanced Manufacturing Technology*** (November 2018).

47. Aseel Jameel Haleel,"Optimization Drilling Parameters of Aluminum Alloy Based on Taguchi Method", ***Al-Khwarizmi Engineerin Journal*** (2018).

48. J. Pradeep Kumar, P. Packiaraj," Effect Of Drilling Parameters On Surface Roughness, Tool Wear, Material Removal Rate And Hole Diameter Error In Drilling Of OHNS", ***International Journal of Advanced Engineering Research and Studies*** (2018).

49. C Sarala Rubi, J Udaya Prakash and C Rajkumar., "Optimization of Process Parameters using Taguchi Technique for Drilling Aluminium Matrix Composites (LM6 / B4C)", ***Materials Science and Engineering*** 912 (2020).

50. Muhammad Aamir, Shanshan Tu, Majid Tolouei-Rad, Khaled Giasin and Ana Vafadar, "Optimization and Modeling of Process Parameters in Multi-Hole Simultaneous Drilling Using Taguchi Method and Fuzzy Logic Approach", ***materials*** (2020).

51. Tarun Sahu and Kamlesh Gangrade.," Optimization of Cutting Parameters to Reduce the Surface Roughness by Taguchi Method", ***International Journal of Research Publication and Reviews*** (2022)

52. Md Shahrukh Khan and Dr. Shahnawaz Alam,“ A Study of the Impact of Multiple drilling parameters on Surface Roughness, Tool wear and Material Removal Rate while Drilling Al6063 applying Taguchi Technique”, ***International Journal of Advanced Engineering Research and Science (IJAERS)***(2022).

53. Internet: ***https://www.machiningdoctor.com/charts/sfm-to-rpm***/ (2022)

54. Internet:***http://www.haascnc.com/tr/machines/vertical-mills/vfseries/models/small/vf-2ss.html*** (2022).

55. Internet: ***http://www.guerrinilauro.it/news-scheda-en.asp?id=16*** (2022).

56. Internet:***https://www.n11.com/urun/1000x-2mp-dijital-standli-8-ledli-usb-otg-mikroskop-21629868?magaza=duhaline*** (2022)

57. Hasan GÖKKAYA and Muammer NALBANT,“ The Effects of Cutting Tool Coating on the Surface Roughness of AISI1015 Steel Depending on Cutting Parameters”, ***Turkish Journal of Engineering and Environmental Sciences*** (2006).

58. Internet: ***https://www.investopedia.com/terms/a/anova.asp*** (2022).

RESUME

Safa Aisa Sasi ALGHATOUS. In 1998 Safa obtained her bachelor’s degree in mechanical engineering department from University of Tripoli, Libya. She began working as a mechanical engineer at the Advanced Center for Technology (ACT) between 1999 and 2020. She is a mechanical design engineer who has held a variety of positions with ACT.